Invariant relativistic kinematics: Phase space triangulation

Jan Hajer

Departamento de Física, Instituto Superior Técnico (IST), Universidade de Lisboa, Avenida Rovisco Pais 1, 1049-001 Lisboa, Portugal

(Received 6 August 2025; accepted 10 September 2025; published 22 October 2025)

The calculation of particle decay widths and scattering cross sections naturally decomposes into a quantum mechanical amplitude and a relativistic phase space (PS). This PS can be formulated in terms of parallelotopes providing frame independent invariants. We demonstrate how these invariants are related to frame dependent observables such as momenta, energies, and angles between particles. Furthermore, we derive expressions for n-dimensional PSs featuring simple integration limits that are particularly well suited for an analytical treatment. To that end we develop a pictorial description using PS diagrams that allow one to straightforwardly identify the optimal set of integration variables for arbitrary n.

DOI: 10.1103/g4ck-sk4s

I. INTRODUCTION

The calculation of scattering cross sections [1,2] and decay widths [3] is a central application of quantum field theory in particle physics [4]. These calculations naturally separate into two parts: the derivation of the quantum mechanical amplitude and the relativistic PS. Since the amplitude encodes the essence of the particle interaction, most publications emphasize its calculation over that of the phase space (PS). In addition, an intuitive pictorial representation of the amplitude in terms of Feynman diagrams is well established [5–7].

After an early period of intensive research on the parametrization of differential PSs [8–15], interest in further development of the topic declined and the kinematics of particle interactions and the construction of PSs are now typically treated in standard textbooks [16–19] and implemented in dedicated computer programs [20–25]. Although there have been attempts to develop diagrammatic tools for PS calculations [26,27], none of these approaches has become widely adopted.

In this work, we aim to bridge this gap by developing a formulation of many-body PSs using only invariant quantities. Naturally, this calculation recovers known results [18]. Beyond these expressions we introduce a parametrization of the PS in terms of angular variables with simple integration limits that is particularly well suited for analytic calculations. To this end, we introduce a pictorial description based on PS diagrams, which encode the essential kinematic information of particle interactions in a geometric and frame independent manner.

We begin in Sec. II by introducing the relativistic PS and provide expressions for the particle decay width and the scattering cross section. We follow up in Sec. III by employing determinants used in distance geometry to compute volumes and angles of parallelotopes in Euclidean space as well as Minkowski spacetime (MST) and relate them to invariants in particle interactions. After establishing these basics we show in Sec. IV how the invariant area of a parallelogram can be used to compute both the frame dependent momenta of particle interactions, as well as the two-body PS. Subsequently, we relate the volume of a parallelepiped to the opening angle between interacting particles and compute the three-body PS in Sec. V. Afterwards we connect the volume of a four-dimensional parallelotope to the angle between two decay planes and compute the four-body PS in Sec. VI. In Sec. VII, we show how the volume of a five-dimensional parallelotope leads to a constraint relevant for the calculation of the five-body PS. This derivation culminates in the generalization of this construction to arbitrary-dimensional PSs in Sec. VIII. Finally, we conclude in Sec. IX.

II. PHASE SPACE

The differential phase space of a relativistic n-body interaction is defined as a function of the four-momenta $\boldsymbol{p}_i = (E_i, \mathsf{p}_i)$ via[1]

Published by the American Physical Society under the terms of the Creative Commons Attribution 4.0 International license. Further distribution of this work must maintain attribution to the author(s) and the published article's title, journal citation, and DOI. Funded by SCOAP³.

[1]We indicate suppressed three- and four-space indices using p and $\boldsymbol{p}$, respectively.

$$d^{3n-4}\Phi_n(\boldsymbol{p}_{a\cdots n};\boldsymbol{p}_a,\ldots,\boldsymbol{p}_n) = \zeta\boldsymbol{p}_{a\cdots n}^2 \iiiint \bar{\delta}^4\left(\boldsymbol{p}_{a\cdots n} - \sum_{i=a}^{n}\boldsymbol{p}_i\right)\prod_{i=a}^{n}\int \bar{\delta}(\zeta\boldsymbol{p}_i^2 - m_i^2)\bar{d}^4\boldsymbol{p}_i, \tag{2.1}$$

where the Dirac distributions place the outgoing particles on-shell and ensure energy-momentum conservation by forcing one of the momenta to be equal to the sum $\boldsymbol{p}_{a\cdots n} = \boldsymbol{p}_a + \cdots + \boldsymbol{p}_n$. The sign of the momentum squares depends on the signature of the metric[2]

$$\zeta = \begin{cases} 1 & \text{Euclidean space and MST with mostly negative metric,} \\ -1 & \text{pseudo-Euclidean space and MST with mostly positive metric,} \end{cases} \tag{2.2}$$

and the barred quantities are normalized with powers of 2π

$$\bar{\delta}^n(x-y) = (2\pi)^n\delta^n(x-y), \qquad \bar{d}^n x = \frac{d^n x}{(2\pi)^n}. \tag{2.3}$$

Since the differential PS can be expressed in terms of invariant masses [9,12,13], we write

$$d^{3n-4}\Phi_n(m_{a\cdots n};m_a,\ldots,m_n) \coloneqq d^{3n-4}\Phi_n(\boldsymbol{p}_{a\cdots n};\boldsymbol{p}_a,\ldots,\boldsymbol{p}_n). \tag{2.4}$$

In order to facilitate a generic notation we use only invariant mass squares

$$\mathfrak{m}_i^2 \coloneqq \zeta\boldsymbol{p}_i^2, \tag{2.5}$$

in place of Mandelstam variables [28]. Throughout, invariant mass squares constructed from unconstrained momenta are denoted by Fraktur symbols $\mathfrak{m}_i$, whereas physical on-shell masses are indicated by the standard notation m_i. In the following we abbreviate the arguments of functions f that depend on $n-i$ independent particles using

$$f(m_{a\cdots i\cdots n}) \coloneqq f(\mathfrak{m}_{a\cdots i},m_{i+1},\ldots,m_n) \coloneqq f(m_{a\cdots i\cdots n};\mathfrak{m}_{a\cdots i},m_{i+1},\ldots,m_n), \tag{2.6}$$

when no disambiguity can arise. Furthermore, the relative orientation of the differential PS (2.4) with respect to a reference frame is relevant. In Sec. IV D we show that the relative orientation of the two-body PS can be defined by the solid angle differential (4.28) by adding two additional particles with masses m_{n+1} and m_{n+2}. This argument is summarized in Fig. 2. As shown in Sec. V C the relative orientation of higher dimensional PSs is defined by the Euler angle differential (5.25) that depends on a third additional particle with mass m_{n+3}. Therefore, we write

$$d^{3n-4}\Phi_n(m_{a\cdots i\cdots n};m_{n+1},\ldots) \coloneqq d^{3n-4}\Phi_n(m_{a\cdots i\cdots n};m_{a\cdots i},m_{i+1},\ldots,m_n;m_{n+1},\ldots). \tag{2.7}$$

A high-dimensional differential PS can be generated from two lower-dimensional differential PSs using the recursion relation [29][3]

$$\begin{aligned} d^{3n-4}\Phi_n(m_{a\cdots n};m_{n+1},\ldots) = 2\frac{\tilde{d}\mathfrak{m}_{a\cdots i}^2}{\mathfrak{m}_{a\cdots i}^2}\, & d^{3i-4}\Phi_i(\mathfrak{m}_{a\cdots i};m_{i+1},\ldots) \\ & d^{3(n-i)-1}\Phi_{n-i+1}(m_{a\cdots n};\mathfrak{m}_{a\cdots i},m_{i+1},\ldots,m_n;m_{n+1},\ldots), \end{aligned} \tag{2.8}$$

where the tilded quantities are normalized with powers of 4π

$$\tilde{\delta}^n(x-y) = (4\pi)^n\,\delta^n(x-y), \quad \tilde{d}^n x = \frac{d^n x}{(4\pi)^n}. \tag{2.9}$$

[2]The pseudo-Euclidean metric contains an overall minus sign in comparison to the Euclidean metric and appears e.g. after a Wick rotation of both of the Lorentzian metrics.

[3]Where we have used that $\delta(a-b) = \int\delta(a-x)\delta(x-b)dx$.

In particular we rely on the recursive factorization into differential two-body PSs via

$$d^{3n-4}\Phi_n(m_{a\cdots n};m_{n+1},\ldots)=d^3\Phi_2'(\mathfrak{m}_{ab};m_c,m_d)d^{3n-7}\Phi_{n-1}(m_{a\cdots n};\mathfrak{m}_{ab},m_c,\ldots,m_n;m_{n+1},\ldots), \tag{2.10}$$

where we have defined the augmented two-body PS differential

$$d^3\Phi_2'(\mathfrak{m}_{ab};m_c,m_d)=2\frac{\eth\mathfrak{m}_{ab}^2}{\mathfrak{m}_{ab}^2}\,d^2\Phi_2(\mathfrak{m}_{ab};m_c,m_d). \tag{2.11}$$

The explicit frame independent expression for the differential two-body PS is derived in Sec. IV E and given in (4.36), while the resulting frame independent expression for the augmented two-body PS differential is given in (6.18). Two different parametrizations of the augmented two-body PS differential are depicted in Fig. 6(b).

A. Decay width and cross section

We define the differential n-body quantum PS as the product of the squared amplitude and the differential n-body PS

$$d^{3n-4}\Psi_n(m_{a\cdots n};m_{n+1},\ldots)=\frac{1}{2}|\mathcal{A}_{n+1}|^2d^{3n-4}\Phi_n(m_{a\cdots n};m_{n+1},\ldots). \tag{2.12}$$

Note that four-momentum conservation restricts the momenta of an $n+1$ particle interaction to an n-body PS. Since the mass dimensions of the amplitude and the PS are $3-n$ and $2n-2$, respectively, the quantum PS has mass-dimension four. The differential decay width of a particle with mass $m_{a\cdots n}$ decaying into n particles is then given by [19]

$$d^{3n-4}\Gamma_n(m_{a\cdots n};m_{n+1},\ldots)=\frac{d^{3n-4}\Psi_n(m_{a\cdots n};m_{n+1},\ldots)}{E_{a\cdots n}(m_{a\cdots n+1})m_{a\cdots n}^2}, \tag{2.13}$$

and has mass dimension one. The energy $E_{a\cdots n}(m_{a\cdots n+1})$ is measured in the rest frame of the observer, defined here as the rest frame of the particle with mass $m_{a\cdots n+1}$. In the rest frame of the decaying particle $m_{a\cdots n+1}\equiv m_{a\cdots n}$ the energy becomes $E_{a\cdots n}(m_{a\cdots n})=m_{a\cdots n}$. See also the discussion around the identities (4.21).

We define the differential cross section of two particles with masses $m_{a\cdots n}$ and m_n scattering into $n-1$ particles by

$$d^{3n-5}\sigma_n(m_{a\cdots n},m_n;m_{a\cdots n-1};m_a,\ldots,m_{n-1};m_{n+1},\ldots)= \pi\int\eth(\mathfrak{m}_{a\cdots n-1}^2-m_{a\cdots n-1}^2)\frac{d^{3n-4}\Psi_n(m_{a\cdots n};m_{n+1},\ldots)}{V_2^2(m_{a\cdots n})}, \tag{2.14}$$

where the Dirac distribution fixes the invariant mass $\mathfrak{m}_{a\cdots n-1}$ to the center-of-momentum (c.m.) energy $m_{a\cdots n-1}$. The square of the area V_2 will be introduced in Sec. IV A and is related to the commonly used Källén triangle function [17] via $V_2^2(m_{a\cdots n})=\lambda(m_{a\cdots n}^2,\mathfrak{m}_{a\cdots n-1}^2,m_n^2)/4$. Since it has mass-dimension four the mass dimension of the cross section is minus two.[4] Note that the momentum of the particle with mass m_n is reversed in comparison to the notation used in the definition of the PS (2.1) and the decay width (2.13). This fact becomes important when calculating quantities that depend on the Gram determinant (3.3), such as the extremal values (5.10) or the cosine of the polar opening angle (5.14) and the cosine of the azimuthal decay plane angle (6.10). Using the recursion relation (2.10) the n-body PS of the cross section can be split into an augmented two-body PS differential (2.11) for the incoming particles and an outgoing $n-1$-body PS. After inserting the explicit expression for the two-body PS (4.37) of the incoming particles and integrating over the corresponding solid angle differential (4.31) as well as the invariant mass differential that corresponds to the c.m. energy, the differential cross sections reads

$$d^{3n-7}\sigma_n(m_{a\cdots n},m_n;m_{a\cdots n-1};m_a,\ldots,m_{n-1};m_{n+1},\ldots) =|\mathcal{A}_{n+1}|^2\frac{d^{3n-7}\Phi_{n-1}(m_{a\cdots n-1};m_n,\ldots)}{4V_2(m_{a\cdots n})m_{a\cdots n-1}^2}, \tag{2.15}$$

where the amplitude contains the complete process, while the differential PS describes only the outgoing part of the process. Furthermore, only one of the integrals over the external Euler angle differential (5.25) remains in this expression and the seemingly external angle differentials in the PS of the final state particles are connected to the incoming particles. The factor $4V_2(m_{a\cdots n})$ in the cross section (2.15) is commonly called the Møller flux factor [30,31].

[4]For practical purposes it is useful to know that $\hbar^2c^2/\mathrm{GeV}^2\approx 0.3894$ mb.

III. DISTANCE GEOMETRY

Four-momentum conservation constrains the Minkowski spacetime physically accessible in an n-body interaction to n-dimensional parallelotopes $\square_n(m_a,\ldots,m_n)$ whose edges are given by the particle masses. Just as in Euclidean space these parallelotopes can be triangulated by simplices $\triangle_n(m_a,\ldots,m_n)$ of the same dimension. Relevant properties of the particle interaction can be identified with angles of these simplices. Since the parallelotopes and simplices are completely defined by their edges, their properties can be derived using determinants of the four-momenta used in distance geometry.

A. Gram and Cayley-Menger determinants

Given $2n$ particles with momenta $\boldsymbol{p}_n$ we use the $4\times n$-dimensional matrices $(\boldsymbol{p}_a,\boldsymbol{p}_b,\ldots,\boldsymbol{p}_n)$ to define the determinant of the n-dimensional Gram matrix [32]

$$G_n^2\begin{pmatrix}\boldsymbol{p}_a,\ldots,\boldsymbol{p}_n\\ \boldsymbol{p}'_a,\ldots,\boldsymbol{p}'_n\end{pmatrix} \coloneqq \zeta^{n+1}\eta\begin{vmatrix}\boldsymbol{p}_a\cdot\boldsymbol{p}'_a & \boldsymbol{p}_a\cdot\boldsymbol{p}'_b & \cdots & \boldsymbol{p}_a\cdot\boldsymbol{p}'_n\\ \boldsymbol{p}_b\cdot\boldsymbol{p}'_a & \boldsymbol{p}_b\cdot\boldsymbol{p}'_b & \cdots & \boldsymbol{p}_b\cdot\boldsymbol{p}'_n\\ \vdots & \vdots & \ddots & \vdots\\ \boldsymbol{p}_n\cdot\boldsymbol{p}'_a & \boldsymbol{p}_n\cdot\boldsymbol{p}'_b & \cdots & \boldsymbol{p}_n\cdot\boldsymbol{p}'_n\end{vmatrix}, \tag{3.1}$$

where the global sign is given by the signature (2.2) and the determinant of the metric

$$\eta=\begin{cases}1 & \text{Euclidean space},\\ -1 & \text{Minkowski spacetime}\end{cases} \tag{3.2}$$

and ensures positivity. The mass dimension of the Gram determinant is $2n$. In the following we single out two particles with momenta $\boldsymbol{p}_a$ and $\boldsymbol{p}_b$ and set for all other momenta $\boldsymbol{p}'_i=\boldsymbol{p}_i$. Since the result can be expressed in terms of mass squares we introduce the notation

$$G_{n-1}^2(m_a,m_b;m_c,\ldots,m_n)\coloneqq\zeta^{n-1}G_{n-1}^2\begin{pmatrix}\boldsymbol{p}_a,\boldsymbol{p}_c,\ldots,\boldsymbol{p}_n\\ \boldsymbol{p}_b,\boldsymbol{p}_c,\ldots,\boldsymbol{p}_n\end{pmatrix}. \tag{3.3}$$

Changing the sign of $\boldsymbol{p}_a$ or $\boldsymbol{p}_b$ as may be necessary for the calculation of the production cross section (2.14) switches the sign of the Gram determinant.

For $n\geq 2$ the Laplace expansion of the Gram determinant along the first column in terms of minors can be written as

$$\eta G_{n-1}^2(m_a,m_b;m_c,\ldots,m_n)=G_1^2(m_a,m_b)V_{n-2}^2(m_c,m_d,\ldots,m_n)-\sum_{i=c}^{n}G_1^2(m_b,m_i)G_{n-2}^2(m_a,m_i;\ldots), \tag{3.4}$$

where the symmetric Gram determinant is defined via

$$V_n^2(m_a,m_b,\ldots,m_n)\coloneqq G_n^2(m_a,m_b;m_b,\ldots,m_n). \tag{3.5}$$

It corresponds to the Cayley-Menger (CM) determinant [33,34] and can therefore be written as a determinant of the $n+2$-dimensional matrix [35,36]

$$V_n^2(m_a,\ldots,m_n)=\frac{(-\eta)^{n+1}}{2^n}\begin{vmatrix}0 & 1 & 1 & 1 & \ldots & 1\\ 1 & 0 & m_a^2 & \mathfrak{m}_{ab}^2 & \ldots & m_{a\cdots n}^2\\ 1 & m_a^2 & 0 & m_b^2 & \ldots & \mathfrak{m}_{b\cdots n}^2\\ 1 & \mathfrak{m}_{ab}^2 & m_b^2 & 0 & \ldots & \mathfrak{m}_{c\cdots n}^2\\ \vdots & \vdots & \vdots & \vdots & \ddots & \vdots\\ 1 & m_{a\cdots n}^2 & \mathfrak{m}_{b\cdots n}^2 & \mathfrak{m}_{c\cdots n}^2 & \ldots & 0\end{vmatrix}, \tag{3.6}$$

where the invariant masses are canonical and defined as in (2.5). Generically, we call invariant masses featuring an uninterrupted and increasing sequence of indices canonical.

B. Invariants in Minkowski spacetime

In four dimensions we define the five contractions of the Levi-Civita (LC) tensor density with zero to four momenta via

$$v_{\mu_{i+1}\ldots\mu_{4-i}}(\boldsymbol{p}_{a_1},\ldots,\boldsymbol{p}_{a_i})=\sqrt{\frac{(\eta\zeta)^{4-i}}{(4-i)!}}\epsilon_{\mu_1\mu_2\mu_3\mu_4}p_{a_1}^{\mu_1}\ldots p_{\mu_i}^{\mu_i}. \tag{3.7}$$

Therefore, in the two extreme cases of the contraction with zero and four momenta the tensor densities read

$$\upsilon_{\mu\nu\rho\sigma} = \sqrt{\frac{(\eta\zeta)^4}{4!}}\epsilon_{\mu\nu\rho\sigma}, \quad \upsilon(\boldsymbol{p}_a,\boldsymbol{p}_b,\boldsymbol{p}_c,\boldsymbol{p}_d) = \epsilon_{\mu\nu\rho\sigma}p_a^\mu p_b^\nu p_c^\rho p_d^\sigma. \tag{3.8}$$

The contraction of two different tensor densities with the same number of free indices can then be expressed using the Gram determinants (3.1). The special case used in the definition (3.3) reads then

$$\upsilon_{\nu\rho\sigma}(\boldsymbol{p}_a)\upsilon^{\nu\rho\sigma}(\boldsymbol{p}_b) = G_1^2(m_a,m_b), \tag{3.9a}$$

$$\upsilon_{\rho\sigma}(\boldsymbol{p}_a,\boldsymbol{p}_b)\upsilon^{\rho\sigma}(\boldsymbol{p}_b,\boldsymbol{p}_c) = G_2^2(m_a,m_b;m_c), \tag{3.9b}$$

$$\upsilon_{\sigma}(\boldsymbol{p}_a,\boldsymbol{p}_c,\boldsymbol{p}_d)\upsilon^{\sigma}(\boldsymbol{p}_b,\boldsymbol{p}_c,\boldsymbol{p}_d) = G_3^2(m_a,m_b;m_c,m_d), \tag{3.9c}$$

$$\upsilon(\boldsymbol{p}_a,\boldsymbol{p}_c,\boldsymbol{p}_d,\boldsymbol{p}_e)\upsilon(\boldsymbol{p}_b,\boldsymbol{p}_c,\boldsymbol{p}_d,\boldsymbol{p}_d) = G_4^2(m_a,m_b;m_c,m_d,m_e). \tag{3.9d}$$

The contraction of two identical tensor densities (3.7) results in CM determinants (3.6) of dimension zero to four

$$\upsilon_{\mu\nu\rho\sigma}\upsilon^{\mu\nu\rho\sigma} = V_0^2, \qquad \upsilon_{\rho\sigma}(\boldsymbol{p}_a,\boldsymbol{p}_b)\upsilon^{\rho\sigma}(\boldsymbol{p}_a,\boldsymbol{p}_b) = V_2^2(m_{ab}), \tag{3.10a}$$

$$\upsilon_{\nu\rho\sigma}(\boldsymbol{p}_a)\upsilon^{\nu\rho\sigma}(\boldsymbol{p}_a) = V_1^2(m_a), \qquad \upsilon_{\sigma}(\boldsymbol{p}_a,\boldsymbol{p}_b,\boldsymbol{p}_c)\upsilon^{\sigma}(\boldsymbol{p}_a,\boldsymbol{p}_b,\boldsymbol{p}_c) = V_3^2(m_{abc}), \tag{3.10b}$$

$$\upsilon(\boldsymbol{p}_a,\boldsymbol{p}_b,\boldsymbol{p}_c,\boldsymbol{p}_d)\upsilon(\boldsymbol{p}_a,\boldsymbol{p}_b,\boldsymbol{p}_c,\boldsymbol{p}_d) = V_4^2(m_{abcd}). \tag{3.10c}$$

The relations between the contractions of the LC tensor densities with the Gram and CM determinants suggests their appearance as invariants in calculations in MST. The fact that the largest CM determinant that can be constructed from the LC tensor density is of dimension four reflects the fact that higher dimensional CM determinants must vanish in such calculations.

C. Volumes of parallelotopes and simplices

The volume $V_n(m_a,\ldots,m_n)$ of an n-dimensional parallelotope $\square_n(m_a,\ldots,m_n)$ with edges m_i and diagonal $m_{a\cdots n}$ is given by the square root of the CM determinant (3.6). Furthermore, an n-dimensional parallelotope is triangulated by $n!$ simplices $\triangle_n(m_a,\ldots,m_n)$ with volumes $V_n(m_a,\ldots,m_n)/n!$. These simplices are defined by the edges m_i, $m_{a\cdots n}$, and additional invariant masses appearing in the CM determinant (3.6). The volumes of the zero- and one-dimensional parallelotopes are

$$V_0 = \sqrt{\eta}, \qquad V_1(m_a) = m_a. \tag{3.11}$$

Due to the sign in the definition (3.1) the Minkowskian volumes differ by a factor of i^{n+1} from Euclidean volumes. Consequently the zero-dimensional volume in (3.11) is imaginary in MST. Additionally, this difference affects the area of the two-dimensional parallelogram $\square_2(m_{ab})$ and the volume of the four-dimensional parallelotope $\square_4(m_{abcd})$. Since the triangle inequality in MST is inverted in comparison to Euclidean space [37]

$$\begin{aligned} &m_a + m_b \geq m_{ab} \quad \text{for Euclidean space,} \\ &m_a + m_b \leq m_{ab} \quad \text{for Minkowski spacetime,} \end{aligned} \tag{3.12}$$

the area of the triangle $\triangle_2(m_{ab};m_a,m_b)$ is defined to be real in MST as well as in Euclidean space. In the following we illustrate parallelotopes and simplices in MST using depictions in Euclidean space, keeping in mind that not all properties are represented adequately. In particular the triangle inequality (3.12) cannot be depicted correctly.

D. Determinant identities

Since invariants in MST can be identified with volumes that are calculated using determinants, relations between these invariants can be constructed from determinant identities. On the one hand, specifying the Laplace expansion of the Gram determinant (3.4) to the symmetric case allows one to express the n-dimensional CM determinant as a function of an $n-1$-dimensional CM determinant and a sum of Gram determinant pairs

$$\eta V_n^2(m_a,\ldots,m_n) = m_a^2 V_{n-1}^2(m_a,\ldots,m_{n-1}) - \sum_{i=b}^{n} G_1^2(m_a,m_i)G_{n-1}^2(m_a,m_i;\ldots). \tag{3.13}$$

On the other hand, applying the Desnanot-Jacobi (DJ) determinant identity[5] to the Gram determinant (3.3) results in

$$\begin{aligned} &G_{n-1}^2(m_a,m_b;m_c\ldots,m_n)V_{n-3}^2(m_d,\ldots,m_n) \\ &= V_{n-2}^2(m_c,\ldots,m_n)G_{n-2}^2(m_a,m_b;m_d\ldots,m_n) \\ &\quad - G_{n-2}^2(m_a,m_c;m_d,\ldots,m_n)G_{n-2}^2(m_b,m_c;m_d,\ldots,m_n), \end{aligned} \tag{3.14}$$

[5]The DJ determinant identity is the two-dimensional version of the Sylvester's determinant identity and reads $\det M \det M_{i,j}^{i,j} = \left|\begin{smallmatrix} \det M_i^i & \det M_i^j \\ \det M_j^i & \det M_j^j \end{smallmatrix}\right|$ where M_i^j corresponds to the submatrix of the matrix M that has the ith row and jth column removed.

and applying it to the symmetric Gram determinant (3.5) gives

$$V_n^2(m_a,\ldots,m_n)V_{n-2}^2(m_c,\ldots,m_n) = \begin{vmatrix} V_{n-1}^2(m_b,m_c,\ldots,m_n) & G_{n-1}^2(m_a,m_b;m_c,\ldots,m_n) \\ G_{n-1}^2(m_a,m_b;m_c,\ldots,m_n) & V_{n-1}^2(m_a,m_c,\ldots,m_n) \end{vmatrix}. \tag{3.15}$$

This determinant can either be expressed as

$$\begin{aligned} &V_n^2(m_a,\ldots,m_n)V_{n-2}^2(m_c,\ldots,m_n) \\ &= V_{n-1}^2(m_a,m_c,\ldots,m_n)V_{n-1}^2(m_b,m_c,\ldots,m_n) \\ &\quad - G_{n-1}^4(m_a,m_b;m_c,\ldots,m_n), \end{aligned} \tag{3.16}$$

or as a two-dimensional CM determinant of further CM determinants

$$\begin{aligned} &- V_n^2(m_a,m_b,m_c,\ldots,m_n)V_{n-2}^2(m_c,\ldots,m_n) \\ &= V_2^2(V_{n-1}(\mathfrak{m}_{ab},m_c,\ldots,m_n);V_{n-1}(m_a,m_c,\ldots,m_n), \\ &\quad V_{n-1}(m_b,m_c,\ldots,m_n)). \end{aligned} \tag{3.17}$$

The properties of the two-dimensional CM determinant V_2^2 will be discussed in more detail in Sec. IV A. A symmetric variant of this expression reads

$$\begin{aligned} &- V_n^2(m_a,m_b,m_c,m_d,\ldots,m_n)V_{n-2}^2(\mathfrak{m}_{abc},m_d,\ldots,m_n) \\ &= V_2^2(V_{n-1}(\mathfrak{m}_{ab},m_c,m_d,\ldots,m_n); \\ &\quad V_{n-1}(\mathfrak{m}_{ac},m_b,m_d,\ldots,m_n),V_{n-1}(\mathfrak{m}_{bc},m_a,m_d,\ldots,m_n)). \end{aligned} \tag{3.18}$$

The noncanonical invariant mass $\mathfrak{m}_{ac}$ appearing here can be expressed in terms of canonical invariant masses using momentum conservation (5.2).

E. Angles of simplices and between particles

An n-dimensional simplex $\triangle_n(m_a,\ldots,m_n)$ has $n+1$ vertices $\kappa_{a\cdots n}^a(\mathfrak{m}_{ab},\ldots,\mathfrak{m}_{a\cdots n-1})$. A characteristic quantity attached to such a vertex is the angle $\alpha_{a\cdots n}^a(\mathfrak{m}_{ab},\ldots,\mathfrak{m}_{a\cdots n-1})$ between the two $n-1$-dimensional simplices $\triangle_{n-1}(m_a,\mathfrak{m}_{ab},\ldots,\mathfrak{m}_{a\cdots n-1})$ and $\triangle_{n-1}(m_{a\cdots n},\mathfrak{m}_{ab},\ldots,\mathfrak{m}_{a\cdots n-1})$. Using the DJ determinant identity (3.16) the cosine of this angle can be calculated to be [18]

$$\cos\alpha_{a\cdots n}^a(\mathfrak{m}_{ab},\ldots,\mathfrak{m}_{a\cdots n-1}) = \frac{G_{n-1}^2(m_{a\cdots n},m_a;\mathfrak{m}_{ab},\ldots,\mathfrak{m}_{a\cdots n-1})}{V_{n-1}(m_{a\cdots n},\mathfrak{m}_{ab},\ldots,\mathfrak{m}_{a\cdots n-1})V_{n-1}(m_a,\mathfrak{m}_{ab},\ldots,\mathfrak{m}_{a\cdots n-1})}, \tag{3.19}$$

while the sine is given by [38]

$$\sin\alpha_{a\cdots n}^a(\mathfrak{m}_{ab},\ldots,\mathfrak{m}_{a\cdots n-1}) = \frac{V_{n-2}(\mathfrak{m}_{ab},\ldots,\mathfrak{m}_{a\cdots n-1})V_n(m_a,\ldots,m_n)}{V_{n-1}(m_{a\cdots n},\mathfrak{m}_{ab},\ldots,\mathfrak{m}_{a\cdots n-1})V_{n-1}(m_a,\mathfrak{m}_{ab},\ldots,\mathfrak{m}_{a\cdots n-1})}. \tag{3.20}$$

While the cosine (3.19) can become negative the sine (3.20) is constrained to be positive for $n>2$, since it consists of a product of volumes. Therefore, the angles that can be described by this pair of equations are constrained to lie within

$$0 \le \alpha_{a\cdots n}^a(\mathfrak{m}_{ab},\ldots,\mathfrak{m}_{a\cdots n-1}) \le \pi. \tag{3.21}$$

In MST these angles can be related to different observables of the involved particles depending on the dimension of the simplex [18].

IV. TWO-BODY INTERACTIONS

Four-momentum conservation ensures that in an interaction of two particles with momenta $\boldsymbol{p}_a$ and $\boldsymbol{p}_b$ the third particle has momentum

$$\boldsymbol{p}_{ab} := \boldsymbol{p}_a + \boldsymbol{p}_b \tag{4.1}$$

and its invariant mass square (2.5) is identical to the mass of the third particle

$$\zeta\boldsymbol{p}_{ab}^2 =: \mathfrak{m}_{ab}^2 = m_{ab}^2, \quad m_{ab}^2 = m_a^2 + m_b^2 + 2\zeta\boldsymbol{p}_a\cdot\boldsymbol{p}_b. \tag{4.2}$$

Consequently, the two-body PS is parametrized by a parallelogram $\square_2(m_{ab};m_a,m_b)$ with edges m_a and m_b. Its diagonal is m_{ab} and it is triangulated by two triangles $\triangle_2(m_{ab};m_a,m_b)$ that are formed by the edges m_a, m_b, and m_{ab}. See Fig. 1(a) for a depiction.

A. Parallelograms and triangles

For two-body processes the Gram determinants (3.3) have mass-dimension two. Using the expansion (4.2) the Gram determinant at the vertex κ_b^a reads

$$G_1^2(m_a,m_b) = \zeta G_1^2\begin{pmatrix}\boldsymbol{p}_a\\ \boldsymbol{p}_b\end{pmatrix} = \zeta\boldsymbol{p}_a\cdot\boldsymbol{p}_b = \frac{m_{ab}^2-m_a^2-m_b^2}{2}. \tag{4.3}$$

Four-momentum conservation (4.1) ensures that two Gram determinants can be added to result in a squared mass

$$G_1^2(m_a, m_{ab}) - G_1^2(m_a, m_b) = m_a^2,$$
$$G_1^2(m_{ab}, m_a) + G_1^2(m_{ab}, m_b) = m_{ab}^2. \tag{4.4}$$

The two-body CM determinant (3.6) has mass dimension four and reads

$$V_2^2(m_{ab}; m_a, m_b) = -\frac{\eta}{4}\begin{vmatrix} 0 & 1 & 1 & 1 \\ 1 & 0 & m_a^2 & m_{ab}^2 \\ 1 & m_a^2 & 0 & m_b^2 \\ 1 & m_{ab}^2 & m_b^2 & 0 \end{vmatrix}. \tag{4.5}$$

Its square root corresponds to the area of the parallelogram $\|_2(m_{ab}; m_a, m_b)$ shown in Fig. 1(a). The area can also be written using Heron's formula [39]

$$V_2^2(m_{ab}; m_a, m_b) = 4\eta t(m_a; m_a, m_b) t(m_b; m_a, m_b) \times t(m_{ab}; m_a, m_b) s(m_{ab}; m_a, m_b), \tag{4.6}$$

where the t function and the semiperimeter s of the triangle are

$$t(m_i; m_a, m_b) := s(m_{ab}; m_a, m_b) - m_i,$$
$$s(m_{ab}; m_a, m_b) := \frac{m_{ab} + m_a + m_b}{2}. \tag{4.7}$$

The corresponding triangle $\triangle_2(m_{ab}; m_a, m_b)$ depicted in Fig. 1(b) has the area $V_2(m_{ab}; m_a, m_b)/2$. The sign η defined in (3.2) ensures that it is real for the Euclidean and the Minkowskian triangle inequality (3.12). Limiting cases for the area of the parallelogram relevant in MST are

$$V_2(m_{ab}; m_a, m_b) = \frac{\sqrt{-\eta}}{2}\begin{cases} m_{ab}\sqrt{m_{ab}^2 - 4m_a^2} & \text{for } m_b = m_a, \\ m_{ab}^2 - m_a^2 & \text{for } m_b = 0, \\ m_{ab}^2 & \text{for } m_b = m_a = 0, \\ 0 & \text{for } m_b = m_{ab} - m_a. \end{cases} \tag{4.8}$$

Hence, the area of the parallelogram $\square_2(m_{ab}; m_a, m_b)$ vanishes when the triangle inequality (3.12) is saturated. Therefore, the physical regime of the two-body interaction (4.1) is characterized by a positive area for this parallelogram. Furthermore, the area can be connected to the Gram determinant (4.3). On the one hand, specifying the DJ determinant identity (3.16) to two dimensions results in

$$\eta V_2^2(m_a, m_b) = m_a^2 m_b^2 - G_1^4(m_a, m_b). \tag{4.9}$$

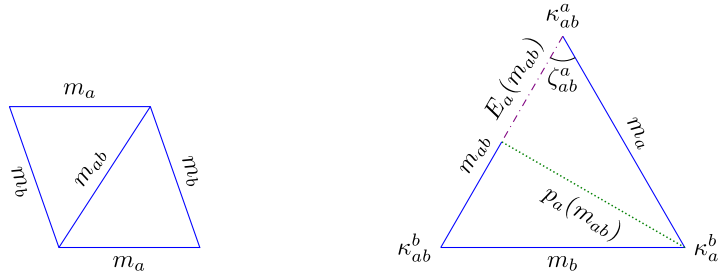
On the other hand specifying the Laplace expansion (3.13) and employing four-momentum conservation (4.4) results in

$$\eta V_2^2(m_a, m_b) = G_1^2(m_a, m_{ab}) G_1^2(m_b, m_{ab}) - m_{ab}^2 G_1^2(m_a, m_b). \tag{4.10}$$

B. Rapidity, Lorentz factor, and velocity norm

In MST the angle at the vertex κ_{ab}^a of the triangle $\triangle_2(m_{ab}; m_a, m_b)$ corresponds to the rapidity ζ_{ab}^a between the rest frames of the particles with masses m_{ab} and m_a; see Fig. 1(b) for a depiction. The (co)sine of this angle can be determined by specifying the generic relations (3.19) and (3.20) to two dimensions

$$\cosh\zeta_{ab}^a = \cos \mathrm{i}\zeta_{ab}^a = \frac{G_1^2(m_a, m_{ab})}{V_1(m_a) V_1(m_{ab})},$$
$$\mathrm{i}\sinh\zeta_{ab}^a = \sin \mathrm{i}\zeta_{ab}^a = \frac{V_0 V_2(m_{ab})}{V_1(m_a) V_1(m_{ab})}. \tag{4.11}$$



(a) PS parallelogram (b) PS diagram with frame dependent quantities

FIG. 1. Two-body PS parallelogram $\square_2(m_{ab}; m_a, m_b)$ in (a) and the PS diagram given by the triangle $\triangle_2(m_a, m_b)$ in (b). (b) Energy $E_a(m_{ab})$ (purple dash-dotted projection) and the absolute values of the momentum $p_a(m_{ab})$ (green dotted height) in the rest frame of the particle with mass m_{ab} as well as the relative rapidity ζ_{ab}^a between these two frames are also indicated; cf. Secs. IV B and IV C. Note that despite this Euclidean depiction the opposite Minkowskian triangle inequality (3.12) must be satisfied in reality.

Here the trigonometric functions are hyperbolic since the volume of the zero-dimensional parallelotope (3.11) is imaginary. Therefore, the rapidity can be expressed as

$$\cosh\zeta^a_{ab} = \frac{G_1^2(m_a, m_{ab})}{m_a m_{ab}}, \qquad \tanh\zeta^a_{ab} = \frac{V_2(m_{ab})}{G_1^2(m_a, m_{ab})},$$
$$\sinh\zeta^a_{ab} = \frac{V_2(m_{ab})}{m_a m_{ab}}, \tag{4.12}$$

where the two-body Gram determinant and the area of the parallelogram are given by (4.3) and (4.5), respectively. The last of these equations constitutes the Minkowskian equivalent to the Euclidean relation that connects the area of a triangle to one of its angles and the lengths of the two adjacent edges. The rapidity is symmetric under exchange of indices and the sum of the angles connected to the longest side is equal to the third angle

$$\zeta^{ab}_a = \zeta^a_{ab}, \qquad \zeta^b_a = \zeta^{ab}_a + \zeta^b_{ab}. \tag{4.13}$$

The hyperbolic trigonometric functions of the rapidity appearing in (4.12) can be identified with the relative Lorentz factor γ^a_{ab} between the two rest frames of the particles with masses m_{ab} and m_a, the corresponding absolute value of the relative velocity called speed $v^a_{ab} := |\mathsf{v}^a_{ab}|$, and their product, the absolute value of the relative proper velocity called celerity

$$\gamma^a_{ab} := \cosh\zeta^a_{ab}, \quad v^a_{ab} := \tanh\zeta^a_{ab}, \quad w^a_{ab} := \gamma^a_{ab} v^a_{ab} = \sinh\zeta^a_{ab}, \tag{4.14}$$

Hence they are given by

$$\gamma^a_{ab} = \frac{G_1^2(m_a, m_{ab})}{m_a m_{ab}}, \qquad v^a_{ab} = \frac{V_2(m_{ab})}{G_1^2(m_a, m_{ab})},$$
$$w^a_{ab} = \frac{V_2(m_{ab})}{m_a m_{ab}}. \tag{4.15}$$

These quantities have the same symmetry as the rapidity (4.13) and obey the addition formulas

$$\gamma^b_a = \gamma^{ab}_a \gamma^b_{ab} + w^{ab}_a w^b_{ab}, \qquad v^b_a = \frac{v^{ab}_a + v^b_{ab}}{1 + v^{ab}_a v^b_{ab}},$$
$$w^b_a = w^{ab}_a \gamma^b_{ab} + \gamma^{ab}_a w^b_{ab}. \tag{4.16}$$

These relations are the usual addition formulas for hyperbolic functions, but can also be derived from the identities (4.9) and (4.10). Using the first of the identities (4.15) the product of two four-momenta appearing in (4.2) can be parametrized in terms of the two corresponding masses and the Lorentz factor between their rest frames

$$\zeta \boldsymbol{p}_a \cdot \boldsymbol{p}_b = m_a m_b \gamma^b_a. \tag{4.17}$$

Therefore, relation (4.2) can be interpreted as the law of cosines for the triangle $\triangle_2(m_{ab}; m_a, m_b)$. The corresponding law of sines is related to the invariant

$$2R(m_{ab}; m_a, m_b) := \frac{m_{ab} m_a m_b}{V_2(m_{ab}; m_a, m_b)} = \frac{m_{ab}}{w^b_a} = \frac{m_a}{w^a_{ab}} = \frac{m_a}{w^a_{ab}}, \tag{4.18}$$

that can be identified with the radius of the circumcircle around the triangle.

C. Energy and three-momentum norm

The energy and the absolute value of the three-momentum $p_a(m_{ab}) := |\mathsf{p}_a(m_{ab})|$ of the particle with mass m_a in the rest frame of particle with mass m_{ab} are expressed via the Lorentz factor and the celerity between these two rest frames (4.14),

$$E_a(m_{ab}) := m_a \gamma^a_{ab}, \qquad p_a(m_{ab}) := m_a w^a_{ab}. \tag{4.19}$$

Therefore, energies and momenta can be interpreted as projections and heights within the triangle $\triangle_2(m_{ab}; m_a, m_b)$, as depicted in Fig. 1(b). Using the identities (4.15) they are given by

$$E_a(m_{ab}) = \frac{G_1^2(m_a, m_{ab})}{m_{ab}}, \quad p_a(m_{ab}) = \frac{V_2(m_{ab})}{m_{ab}}. \tag{4.20}$$

Consequently, the identities

$$E_a(m_a) = m_a, \qquad m_b E_a(m_b) = m_a E_b(m_a), \tag{4.21a}$$

$$p_a(m_a) = 0, \qquad m_b p_a(m_b) = m_a p_b(m_a),$$
$$p_a(m_{ab}) = p_b(m_{ab}) \tag{4.21b}$$

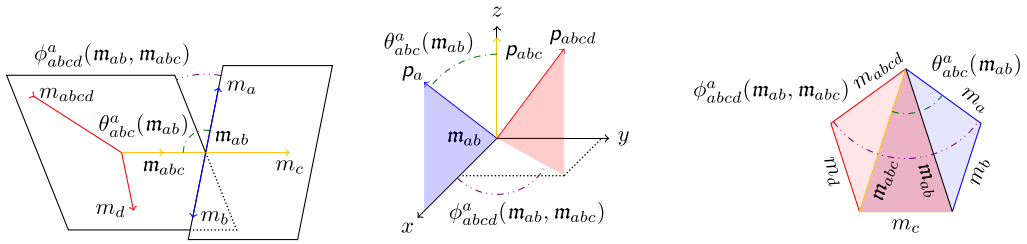
can be directly extracted from the relations (4.20) and Fig. 1(b). Expressing the DJ determinant identity (4.9) in terms of energy and momentum shows that the Pythagorean theorem corresponds to the energy-momentum relation

$$m_a^2 = E_a^2(m_{ab}) + \eta p_a^2(m_{ab}). \tag{4.22}$$

The momentum product appearing in (4.2) can also be formulated frame dependently using these quantities together with the opening angle $\theta^b_a(m_{ab})$ between the particles with mass m_a and m_b in the rest frame of the particle with mass m_{ab},

$$\zeta \boldsymbol{p}_a \cdot \boldsymbol{p}_b = E_a(m_{ab}) E_b(m_{ab}) + \eta p_a(m_{ab}) p_b(m_{ab}) \cos\theta^b_a(m_{ab}). \tag{4.23}$$

The comparison with the parametrization (4.17) results for the cosine of the opening angle in



(a) Decay planes (b) Coordinate system (c) PS diagram

FIG. 2. Angular variables appearing in a four-body process in the rest frame of the invariant mass $\mathfrak{m}_{ab}$ in (a), resulting spherical coordinate system in (b), and the corresponding invariant description in (c). In the rest frame of the invariant mass $\mathfrak{m}_{ab}$ the particles with masses m_a and m_b are back-to-back (4.24). Only after the introduction of another particle with mass m_c that is itself back-to-back with $\mathfrak{m}_{abc}$ it is possible to define a polar opening angle $\theta^a_{abc}(\mathfrak{m}_{ab})$ between these pairs (5.18). In order to define an azimuthal angle $\phi^a_{abcd}(\mathfrak{m}_{ab},\mathfrak{m}_{abc})$ between two planes (6.10) a further particle with mass m_d is necessary. Together these angles define the solid angle of the two-body process of m_a and m_b with respect to the reference frame defined by m_c and m_d.

$$\cos\theta^b_a(m_{ab}) = \eta\frac{m_a m_b\gamma^b_a - E_a(m_{ab})E_b(m_{ab})}{p_a(m_{ab})p_b(m_{ab})} = \eta. \quad (4.24)$$

Therefore, in MST the particles with masses m_a and m_b are back-to-back in the rest frame of the particle with mass m_{ab}. This expression can be interpreted as a degenerate case of the spherical law of cosines (5.18) introduced in Sec. V B.

D. On-shell four-momentum and solid angle differential

The n-body PS (2.1) depends on n four-momentum differentials that are constrained to be on-shell. In order to express the constrained four-momentum differential for $\boldsymbol{p}_a$ when it depends on a reference frame another particle with mass m_b has to be introduced. In the rest frame of their invariant mass $\mathfrak{m}_{ab}$ the constrained four-momentum differential reads

$$\int \eth(\zeta\boldsymbol{p}_a^2 - m_a^2)\mathrm{d}^4\boldsymbol{p}_a = \int \eth(E_a^2(\mathfrak{m}_{ab}) + \eta\mathsf{p}_a^2(\mathfrak{m}_{ab}) - m_a^2)\mathrm{d}E_a(\mathfrak{m}_{ab})\mathrm{d}^3\mathsf{p}_a(\mathfrak{m}_{ab}) = \frac{\mathrm{d}^3\mathsf{p}_a(\mathfrak{m}_{ab})}{2E_a(\mathfrak{m}_{ab})}. \quad (4.25)$$

By extending the reference frame with two more particles, as depicted in Fig. 2, the components of the three-momentum can be expressed using angular variables

$$p^x_a(\mathfrak{m}_{ab};\mathfrak{m}_{abc};\mathfrak{m}_{abcd}) = p_a(\mathfrak{m}_{ab})\sin\theta^a_{abc}(\mathfrak{m}_{ab})\cos\phi^a_{abcd}(\mathfrak{m}_{ab},\mathfrak{m}_{abc}), \quad (4.26a)$$

$$p^y_a(\mathfrak{m}_{ab};\mathfrak{m}_{abc};\mathfrak{m}_{abcd}) = p_a(\mathfrak{m}_{ab})\sin\theta^a_{abc}(\mathfrak{m}_{ab})\sin\phi^a_{abcd}(\mathfrak{m}_{ab},\mathfrak{m}_{abc}), \quad (4.26b)$$

$$p^z_a(\mathfrak{m}_{ab};\mathfrak{m}_{abc};\mathfrak{m}_{abcd}) = p_a(\mathfrak{m}_{ab})\cos\theta^a_{abc}(\mathfrak{m}_{ab}). \quad (4.26c)$$

In the rest frame of $\mathfrak{m}_{ab}$ the polar angle $\theta^a_{abc}(\mathfrak{m}_{ab})$ measures the opening angle between the pair p_a and p_b and the pair p_c and p_{abc}, both of which are back-to-back (4.24). Since the polar opening angle is a property of the three-body system it will be discussed in Sec. V B. The definition of the azimuthal angle requires the introduction of a further particle to the reference frame. The angle between the two planes defined in Fig. 2 is given by the azimuthal angle $\phi^a_{abcd}(\mathfrak{m}_{ab},\mathfrak{m}_{abc})$. Since the azimuthal decay plane angle appears in a four-body system it will be discussed in Sec. VI B.

Therefore, the three-momentum differential appearing in (4.25) can be written as[6]

$$\begin{aligned}\eth^3\mathsf{p}_a(\mathfrak{m}_{ab}) &= 4\,p^2(\mathfrak{m}_{ab})\,\eth p_a(\mathfrak{m}_{ab})\,\eth^2\Omega^a_{abcd}(\mathfrak{m}_{ab};\mathfrak{m}_{abc})\\ &= 4\,E_a(\mathfrak{m}_{ab})\,p_a(\mathfrak{m}_{ab})\,\eth E_a(\mathfrak{m}_{ab})\,\eth^2\Omega^a_{abcd}(\mathfrak{m}_{ab};\mathfrak{m}_{abc}),\end{aligned} \quad (4.27)$$

where the solid angle differential is defined as

$$\eth^2\Omega^a_{abcd}(\mathfrak{m}_{ab};\mathfrak{m}_{abc}) = \sin\theta^a_{abc}(\mathfrak{m}_{ab})\,\eth\theta^a_{abc}(\mathfrak{m}_{ab})\,\eth\phi^a_{abcd}(\mathfrak{m}_{ab},\mathfrak{m}_{abc}). \quad (4.28)$$

[6]Note the transition from the normalization (2.3) to the normalization (2.9).

with[7]

$$\sin\theta^a_{abc}(m_{ab})\;\eth\theta^a_{abc}(m_{ab}) = -\,\eth\cos\theta^a_{abc}(m_{ab}). \tag{4.29}$$

These angles are defined over the domain

$$-1 \le \cos\theta^a_{abc}(m_{ab}) \le 1, \qquad 0 \le \phi^a_{abcd}(m_{ab}, m_{abc}) \le 2\pi. \tag{4.30}$$

Due to the normalization (2.9) they integrate to

$$\int \eth\cos\theta^a_{abc}(m_{ab}) = \frac{1}{2\pi}, \quad \int \eth\phi^a_{abcd}(m_{ab}, m_{abc}) = \frac{1}{2}, \quad \iint \eth^2\Omega^a_{abcd}(m_{ab}; m_{abc}) = \frac{1}{4\pi}. \tag{4.31}$$

The solid angle differential is depicted in two different parametrizations in Fig. 6(a). Using the frame independent formulation of the energy and the absolute value of the three-momentum (4.20) the constrained four-momentum differential (4.25) can therefore be expressed as

$$\int \bar{\delta}(\zeta \boldsymbol{p}_a^2 - m_a^2)\;\bar{d}^4\boldsymbol{p}_a = 2\frac{V_2(m_{ab})}{m_{ab}^2}\;\eth G_1^2(m_a, m_{ab})\;\eth^2\Omega^a_{abcd}(m_{ab}; m_{abc}). \tag{4.32}$$

E. Two-body phase space

Specifying the generic definition of the differential PS (2.1) to two particles

$$d^2\Phi_2(\boldsymbol{p}_{ab};\boldsymbol{p}_a,\boldsymbol{p}_b) = \zeta\boldsymbol{p}_{ab}^2 \iiiint \bar{\delta}^4(\boldsymbol{p}_{ab} - \boldsymbol{p}_a - \boldsymbol{p}_b) \int \bar{\delta}(\zeta\boldsymbol{p}_b^2 - m_b^2)\,\bar{d}^4\boldsymbol{p}_b \int \bar{\delta}(\zeta\boldsymbol{p}_a^2 - m_a^2)\,\bar{d}^4\boldsymbol{p}_a, \tag{4.33}$$

and using the four-dimensional Dirac distribution to integrate over the four-momentum of the second particle results in

$$d^2\Phi_2(\boldsymbol{p}_{ab};\boldsymbol{p}_a, \qquad m_b) = \zeta\boldsymbol{p}_{ab}^2 \int \delta(\zeta(\boldsymbol{p}_{ab} - \boldsymbol{p}_a)^2 - m_b^2) \int \bar{\delta}(\zeta\boldsymbol{p}_a^2 - m_a^2)\,\bar{d}^4\boldsymbol{p}_a. \tag{4.34}$$

Using the constrained four-momentum differential (4.32) of the first particle the differential PS reads

$$\begin{aligned} d^2\Phi_2(m_{ab}; m_a, m_b; m_c, m_d) = {} & V_2(m_{ab})\;\eth^2\Omega^a_{abcd}(m_{ab}; m_{abc}) \\ & 2\int \bar{\delta}\big(m_{ab}^2 - 2\,G_1^2(m_a, m_{ab}) + m_a^2 - m_b^2\big)\;\eth G_1^2(m_a, m_{ab}). \end{aligned} \tag{4.35}$$

Finally, the integral over the Gram determinant results for the differential PS in

$$d^2\Phi_2(m_{ab}; m_c, m_d) = V_2(m_{ab})\;\eth^2\Omega^a_{abcd}(m_{ab}; m_{abc}). \tag{4.36}$$

After integrating over the external solid angle differential (4.31), the PS is constant and frame independent

$$\Phi_2(m_{ab}) = \frac{V_2(m_{ab})}{4\pi}. \tag{4.37}$$

Hence the PS of the interactions between a particle with mass m_{ab} and two particles with masses m_a and m_b is governed by the area of the parallelogram $\square_2(m_{ab}; m_a, m_b)$ depicted in Fig. 1(a). The trivial PS diagram of the two-body PS is depicted in Fig. 1(b).

[7]In the following we will neglect the sign that appears when the differential of a cosine is introduced and assume that it is absorbed in a swap of the integration limits.

F. Decays into two final particles

After the integration over the solid angle differential, the two-body PS (4.37) leads for the decay width (2.13) of a particle with mass m_{ab} that decays into two particles with masses m_a and m_b in its own rest frame to

$$\Gamma_2(m_{ab};m_a,m_b)=\frac{|\mathcal{A}_3|^2}{8\pi}\frac{V_2(m_{ab})}{m_{ab}^3}, \tag{4.38}$$

with the Lagrangian and amplitude of the trivial interaction of three scalar particles

$$\mathcal{L}_3 \supset \frac{g}{3!}\phi_{ab}\phi_a\phi_b, \qquad \mathcal{A}_3=\mathrm{i}g, \tag{4.39}$$

where the coupling constant g has mass dimension one, the decay width reaches for $m_a=m_b=0$ the maximal value of

$$\Gamma_2^{\max}(m_{ab})=\frac{g^2}{16\pi m_{ab}}. \tag{4.40}$$

V. THREE-BODY INTERACTIONS

The invariant mass (2.5) of three particles

$$m_{abc}^2=\mathfrak{m}_{abc}^2\coloneqq\zeta\boldsymbol{p}_{abc}^2, \qquad \boldsymbol{p}_{abc}\coloneqq\boldsymbol{p}_a+\boldsymbol{p}_b+\boldsymbol{p}_c \tag{5.1}$$

can be expressed in terms of the invariant masses of two particles (4.2) via

$$m_{abc}^2=\mathfrak{m}_{ab}^2+\mathfrak{m}_{bc}^2+\mathfrak{m}_{ac}^2-m_a^2-m_b^2-m_c^2, \tag{5.2}$$

and allows one to eliminate the noncanonical invariant mass $\mathfrak{m}_{ac}$. The three-body PS is governed by the volume $V_3(m_{abc};m_a,m_b,m_c)$ of a three-dimensional parallelepiped $\square_3(m_{abc};m_a,m_b,m_c)$. It can be triangulated by six tetrahedra $\triangle_3(m_{abc};m_a,m_b,m_c)$ with volumes $V_3/6$. The freedom to eliminate one of the three two-particle invariant masses results in three different triangulations, only one of which we call canonical. The rapidities, velocities, and Lorentz factors between the different rest frames as well as the energies and momenta in the different rest frames can be derived by calculating the angles, heights, and projections on the different faces of the tetrahedra as demonstrated in Secs. IV B and IV C, respectively.

A. Parallelepipeds and tetrahedra

The three-body Gram determinant (3.3) has mass-dimension four. At the vertex $\kappa^a_{abc}(\mathfrak{m}_{ab})$ between the masses m_{abc} and m_a and the invariant mass $\mathfrak{m}_{ab}$ it is given by

$$G_2^2(m_a,m_{abc};\mathfrak{m}_{ab})=G_2^2\begin{pmatrix}\boldsymbol{p}_a,\boldsymbol{p}_{ab}\\ \boldsymbol{p}_{abc},\boldsymbol{p}_{ab}\end{pmatrix}=\eta\begin{vmatrix}\boldsymbol{p}_a\cdot\boldsymbol{p}_{abc} & \boldsymbol{p}_a\cdot\boldsymbol{p}_{ab}\\ \boldsymbol{p}_{ab}\cdot\boldsymbol{p}_{abc} & \boldsymbol{p}_{ab}\cdot\boldsymbol{p}_{ab}\end{vmatrix}, \tag{5.3}$$

and a Laplace expansion in terms of minors (3.4) leads to

$$\eta G_2^2(m_a,m_{abc};\mathfrak{m}_{ab})=G_1^2(m_a,m_{abc})\mathfrak{m}_{ab}^2-G_1^2(m_a,\mathfrak{m}_{ab})G_1^2(m_{abc},\mathfrak{m}_{ab}). \tag{5.4}$$

The three-body CM determinant (3.6) has mass-dimension six and reads

$$V_3^2(m_{abc};m_a,m_b,m_c)=\frac{1}{8}\begin{vmatrix}0 & 1 & 1 & 1 & 1\\ 1 & 0 & m_a^2 & \mathfrak{m}_{ab}^2 & m_{abc}^2\\ 1 & m_a^2 & 0 & m_b^2 & \mathfrak{m}_{bc}^2\\ 1 & \mathfrak{m}_{ab}^2 & m_b^2 & 0 & m_c^2\\ 1 & m_{abc}^2 & \mathfrak{m}_{bc}^2 & m_c^2 & 0\end{vmatrix}. \tag{5.5}$$

Limiting cases of the volume of the parallelepiped are

$$V_3(m_{abc};m_a,m_b,m_c)=\frac{1}{2}\begin{cases}\mathfrak{m}_{ab}\mathfrak{m}_{bc}\mathfrak{m}_{ac} & \text{for } m_a=m_b=m_c=0,\\ 0 & \text{for } m_{abc}=m_a+m_b+m_c,\\ 0 & \text{for } \mathfrak{m}_{bc}=\mathfrak{m}_{bc}^{\max/\min}(\mathfrak{m}_{ab}).\end{cases} \tag{5.6}$$

Since the volume vanishes if the masses m_a, m_b, and m_c add up exactly to the mass m_{abc}, the physical regime of the three-body process corresponds to positive volumes for the parallelepiped $\square_3(m_{abc};m_a,m_b,m_c)$. Using the DJ determinant identity (3.18) the volume can be compactly written as

$$V_3^2(m_a,m_b,m_c)=-\frac{V_2^2(V_2(\mathfrak{m}_{ac},m_b);V_2(\mathfrak{m}_{ab},m_c),V_2(\mathfrak{m}_{bc},m_a))}{m_{abc}^2}. \tag{5.7}$$

From the two-body limits (4.8) follows then that the volume of the parallelepiped vanishes when the areas of the sides obey

$$V_2(\mathfrak{m}_{ac},m_b)=V_2(\mathfrak{m}_{ab},m_c)+V_2(\mathfrak{m}_{bc},m_a). \tag{5.8}$$

This condition can be exploited to calculate a further constellation that results in a vanishing volume for any masses that obey $m_a+m_b+m_c<m_{abc}$. It is reached when the invariant mass $\mathfrak{m}_{bc}$ assumes as a function of the invariant mass $\mathfrak{m}_{ab}$ one of its extremal values.

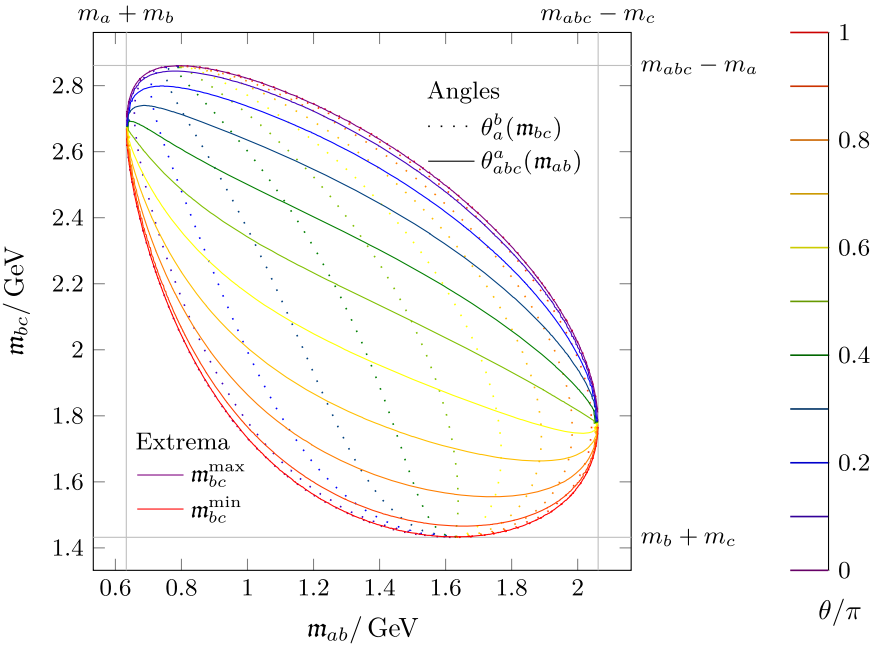


FIG. 3. Dalitz plot of the integration limits (5.9) for the masses $m_a = 139$ MeV, $m_b = 494$ MeV, $m_c = 938$ MeV, $m_{abc} = 3$ GeV, corresponding to a resonance of 3 GeV that decays into $p\bar{K}^0\pi^+$. The allowed region is covered by lines of constant polar opening angles (5.14).

The extrema can be observed in the Dalitz plot [40] shown in Fig. 3 and are given by

$$\mathfrak{m}_{bc}^{\max/\min 2}(\mathfrak{m}_{ab}) = E_{bc}^{+}(\mathfrak{m}_{ab})^2 + \eta p_{bc}^{\pm}(\mathfrak{m}_{ab})^2, \tag{5.9}$$

where the sum of energies and the sum and difference of momenta in the rest frame of the invariant mass $\mathfrak{m}_{ab}$ are given by

$$\begin{aligned} E_{bc}^{+}(\mathfrak{m}_{ab}) &= E_b(\mathfrak{m}_{ab}) + E_c(\mathfrak{m}_{ab}), \\ p_{bc}^{\pm}(\mathfrak{m}_{ab}) &= p_b(\mathfrak{m}_{ab}) \pm \eta p_c(\mathfrak{m}_{ab}). \end{aligned} \tag{5.10}$$

Since the invariant description of the energy (4.20) depends on the Gram determinant (4.3) the sum in the definition of the energy (5.10) can become a difference when calculating the production cross section if one of the four-momenta corresponds to the incoming particle with swapped momentum. A Euclidean depiction of these quantities is shown in Fig. 4(a). In contrast to Euclidean space, in MST the momentum difference results in the minimal invariant mass while the momentum sum leads to the maximal invariant mass. The volume is then given as a function of these extrema as

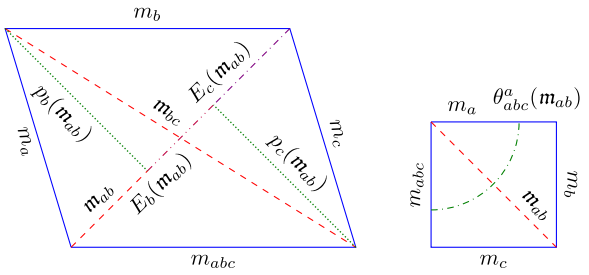
$$\begin{aligned} V_3^2(m_a, m_b, m_c) = &\frac{\mathfrak{m}_{bc}^{\max 2}(\mathfrak{m}_{ab}) - \mathfrak{m}_{bc}^2}{2} \\ &\times \mathfrak{m}_{ab}^2 \frac{\mathfrak{m}_{bc}^2 - \mathfrak{m}_{bc}^{\min 2}(\mathfrak{m}_{ab})}{2}. \end{aligned} \tag{5.11}$$

Specifying the Laplace expansion (3.13) to the three-dimensional case shows that the volumes and Gram determinants are connected via

$$\begin{aligned} \eta V_3^2(m_a, m_b, m_c) = &m_a^2 V_2^2(m_b, m_c) \\ &- G_1^2(m_a, m_b) G_2^2(m_a, m_b; m_c) \\ &- G_1^2(m_a, m_c) G_2^2(m_a, m_c; m_b). \end{aligned} \tag{5.12}$$

B. Opening angle between two particles

The opening angle between the particles with masses m_a and m_{abc} in the rest frame of the invariant mass $\mathfrak{m}_{ab}$



(a) Invariant masses (b) Angular variables

FIG. 4. Diagrams of the three-body PS parametrized using invariant masses (5.30) in (a) and angular variables (5.27) in (b). As indicated by the intersecting invariant masses appearing in (a) the integration limits in this parametrization are nontrivial (5.9). Therefore, we have additionally indicated the quantities that enter the integration limits (5.10) for the integral over $\mathfrak{m}_{bc}$.

$$\cos^a_{abc}(\mathfrak{m}_{ab}) := \frac{\mathsf{p}_a(\mathfrak{m}_{ab}) \cdot \mathsf{p}_{abc}(\mathfrak{m}_{ab})}{|\mathsf{p}_a(\mathfrak{m}_{ab})||\mathsf{p}_{abc}(\mathfrak{m}_{ab})|} \tag{5.13}$$

can be identified with the dihedral angle of the tetrahedron $\triangle_3(m_{abc}; m_a, m_b, m_c)$ at the edge $\mathfrak{m}_{ab}$ when it forms a vertex $\kappa^a_{abc}(\mathfrak{m}_{ab})$ with m_a and m_{abc} [9]. Specifying the general expression for the cosine (3.19) to the three-dimensional case results in the spherical law of cosines

$$\cos\theta^a_{abc}(\mathfrak{m}_{ab}) = \frac{G_2^2(m_a, m_{abc}; \mathfrak{m}_{ab})}{V_2(m_a, \mathfrak{m}_{ab}) V_2(m_{abc}, \mathfrak{m}_{ab})}, \tag{5.14}$$

where the Gram determinant can be expressed by the Laplace expansion (5.4). This expression can then be solved for the invariant mass

$$\mathfrak{m}^2_{bc} = m^2_{abc} + m^2_a - 2\frac{g^a_{abc}(\mathfrak{m}_{ab})}{\mathfrak{m}^2_{ab}}, \tag{5.15}$$

where

$$\begin{aligned} g^a_{abc}(\mathfrak{m}_{ab}) = {} & \eta V_2(m_{abc}, \mathfrak{m}_{ab}) V_2(m_a, \mathfrak{m}_{ab}) \cos\theta^a_{abc}(\mathfrak{m}_{ab}) \\ & + G_1^2(m_{abc}, \mathfrak{m}_{ab}) G_1^2(m_a, \mathfrak{m}_{ab}) \end{aligned} \tag{5.16}$$

and the derivative with respect to the polar opening angle reads

$$\frac{d\mathfrak{m}^2_{bc}}{d\cos\theta^a_{abc}(\mathfrak{m}_{ab})} = -2\eta \frac{V_2(m_{abc}, \mathfrak{m}_{ab}) V_2(m_a, \mathfrak{m}_{ab})}{\mathfrak{m}^2_{ab}}. \tag{5.17}$$

Using the Laplace expansion of the Gram determinant (5.4) and the invariant expressions for the energy and the momenta (4.20) allows to express the cosine of the opening angle (5.14) as function of energies and momenta

$$\cos\theta^a_{abc}(\mathfrak{m}_{ab}) = \eta \frac{m_{abc} E_a(m_{abc}) - E_{abc}(\mathfrak{m}_{ab}) E_a(\mathfrak{m}_{ab})}{p_{abc}(\mathfrak{m}_{ab}) p_a(\mathfrak{m}_{ab})}. \tag{5.18}$$

Using the relation between the energy and the Lorentz factor (4.19) this expression can be compared to the degenerate case (4.24). The sine of the polar opening angle between the particles with masses m_{abc} and m_a in the rest frame of the invariant mass $\mathfrak{m}_{ab}$ is given by specifying the general definition (3.20) to three dimensions

$$\sin\theta^a_{abc}(\mathfrak{m}_{ab}) = \frac{\mathfrak{m}_{ab} V_3(m_{abc}; m_a, m_b, m_c)}{V_2(m_{abc}, \mathfrak{m}_{ab}) V_2(m_a, \mathfrak{m}_{ab})}. \tag{5.19}$$

Therefore, the tangent of the polar opening angle is independent of the two-dimensional volumes

$$\tan\theta^a_{abc}(\mathfrak{m}_{ab}) = \frac{\mathfrak{m}_{ab} V_3(m_{abc}; m_a, m_b, m_c)}{G_2^2(m_a, m_{abc}; \mathfrak{m}_{ab})}. \tag{5.20}$$

According to the spherical law of sines the combinations

$$\begin{aligned} \frac{\sin\theta^a_{abc}(\mathfrak{m}_{ab})}{w^a_{abc}} = \frac{\sin\theta^a_{ab}(m_{abc})}{w^a_{ab}} = \frac{\sin\theta^{ab}_{abc}(m_a)}{w^{ab}_{abc}} \\ = I_1(\mathfrak{m}_{ab}, \mathfrak{m}_{bc}) \end{aligned} \tag{5.21}$$

corresponds to a dimensionless invariant with the value

$$I_1(\mathfrak{m}_{ab}, \mathfrak{m}_{bc}) = \frac{m_a \mathfrak{m}_{ab} m_{abc} V_3(m_{abc}; m_a, m_b, m_c)}{V_2(m_{abc}, \mathfrak{m}_{ab}) V_2(m_a, \mathfrak{m}_{ab}) V_2(m_{abc}, m_a)}. \tag{5.22}$$

C. Three-body phase space

Using the recursion relation (2.10) the differential three-body PS can be constructed from a pair of two-body PSs

$$\begin{aligned} & d^5\Phi_3(m_{abc}; m_a, m_b, m_c; m_d, m_e) \\ & = d^2\Phi_2(m_{abc}; \mathfrak{m}_{ab}, m_c; m_d, m_e) d^3\Phi'_2(\mathfrak{m}_{ab}; m_a, m_b). \end{aligned} \tag{5.23}$$

With the explicit expression of the augmented two-body PS differential (2.11) and the differential two-body PS (4.36) the differential three-body PS reads [19]

$$\begin{aligned} d^5\Phi_3(m_{abc}; m_a, m_b, m_c; m_d, m_e) = {} & 2\, V_2(m_{abc}) \frac{V_2(\mathfrak{m}_{ab})}{\mathfrak{m}^2_{ab}}\, \eth\mathfrak{m}^2_{ab} \\ & \eth^2\Omega^a_{abcd}(\mathfrak{m}_{ab}; m_{abc})\, \eth^2\Omega^{ab}_{abcde}(m_{abc}; \mathfrak{m}_{abcd}), \end{aligned} \tag{5.24}$$

The product of the two solid angle differentials (4.28) can then be expressed as an internal polar opening angle differential (4.29) and an external Euler angle differential

$$\eth^3\Omega^{a;ab}_{abcde;abcd}(m_{abc}) = \eth\phi^a_{abcd}(\mathfrak{m}_{ab}, m_{abc})\, \eth^2\Omega^{ab}_{abcde}(m_{abc}; \mathfrak{m}_{abcd}), \tag{5.25}$$

that captures the orientation of the process in three-space and using the integrals (4.31) integrates to

$$\iiint \eth^3 \Omega^{a;ab}_{abcde;abcd}(m_{abc}) = \frac{1}{8\pi}. \tag{5.26}$$

The Euler angle differential (5.25) is symmetric under the simultaneous exchange of m_a with $\mathfrak{m}_{abcde}$ and $\mathfrak{m}_{ab}$ with $\mathfrak{m}_{abcd}$ as can be seen in the two different parametrizations depicted in Fig. 7. Finally, the differential three-body PS reads

$$d^5\Phi_3(m_{abc}; m_d, m_e) = 2\, V_2(m_{abc}) \frac{V_2(\mathfrak{m}_{ab})}{\mathfrak{m}^2_{ab}}\, \eth \mathfrak{m}^2_{ab}\, \eth \cos\theta^a_{abc}(\mathfrak{m}_{ab})\, \eth^3 \Omega^{a;ab}_{abcde;abcd}(m_{abc}), \tag{5.27}$$

after integrating over the external Euler angle differential (5.26) it becomes

$$d^2\Phi_3(m_{abc}) = \frac{V_2(m_{abc})}{4\pi} \frac{V_2(\mathfrak{m}_{ab})}{\mathfrak{m}^2_{ab}}\, \eth \mathfrak{m}^2_{ab}\, \eth \cos\theta^a_{abc}(\mathfrak{m}_{ab}), \tag{5.28}$$

where the two-body integration limits (4.8) are given by

$$\mathfrak{m}^{\min}_{ab} = m_a + m_b, \qquad \mathfrak{m}^{\max}_{ab} = m_{abc} - m_c. \tag{5.29}$$

The diagram of the three-body PS in this parametrization is presented in Fig. 4(b). Using the differential of the spherical law of cosines (5.17) it is possible to rewrite the differential three-body PS (5.27) as[8]

$$d^5\Phi_3(m_{abc}; m_d, m_e) = \eth \mathfrak{m}^2_{ab}\, \eth \mathfrak{m}^2_{bc}\, \eth^3 \Omega^{a;ab}_{abcde;abcd}(m_{abc}). \tag{5.30}$$

Hence, when parametrizing the differential three-body PS with invariant mass squares it is constant. After integrating over the external Euler angle differential (5.26) the differential three-body PS reads

$$d^2\Phi_3(m_{abc}) = \frac{1}{8\pi}\, \eth \mathfrak{m}^2_{ab}\, \eth \mathfrak{m}^2_{bc}. \tag{5.31}$$

The three-body integration limits (5.9) of the integration over $\mathfrak{m}_{bc}$ are given as a function of $\mathfrak{m}_{ab}$. The remaining two-body integration limits are given by (5.29). The diagram of the three-body PS in this parametrization is shown together with the quantities (5.10) that enter the integration limits (5.9) in Fig. 4(a).

D. Three-body processes

In the following we calculate a decay into three final particles and the two-particle scattering into two final particles using the trivial interaction between four scalar particles with Lagrangian and amplitude

$$\mathcal{L}_4 \supset \frac{\lambda}{4!}\phi_{abc}\phi_a\phi_b\phi_c, \qquad \mathcal{A}_4 = \mathrm{i}\lambda, \tag{5.32}$$

in the limit of massless colliding and final state particles.

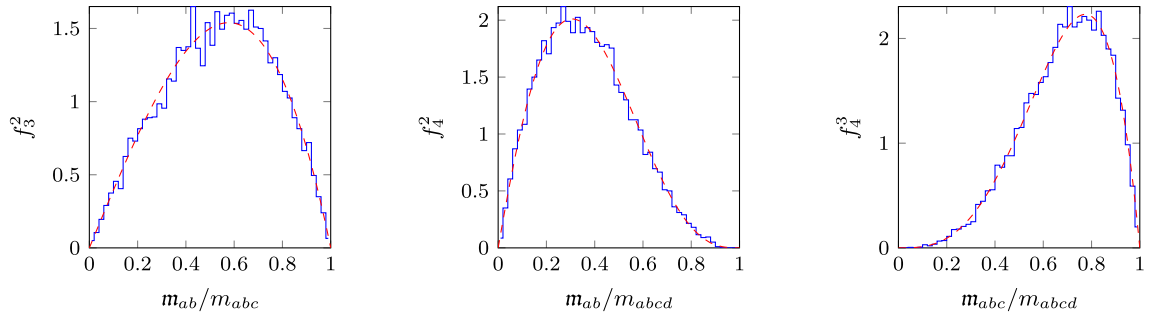
1. Decays into three final particles

Using either of the parametrizations of the three-body PS after the integration over the external Euler angle differential (5.28) and (5.31) together with the trivial amplitude (5.32) in order to specify the differential decay width (2.13) to three-body decays allows one to calculate the decay of a particle with mass m_{abc} into three final state particles in the rest frame of the decaying particle as a function of an angle and an invariant mass

$$d^2\Gamma_3(m_{abc}) = \frac{|\mathcal{A}_4|^2}{8\pi} \frac{V_2(m_{abc})}{m^3_{abc}} \frac{V_2(\mathfrak{m}_{ab})}{\mathfrak{m}^2_{ab}}\, \eth \mathfrak{m}^2_{ab}\, \eth \cos\theta^a_{abc}(\mathfrak{m}_{ab}), \tag{5.33}$$

or alternatively as a function of two invariant masses

[8]We compensate any sign that might appear in the PSs by swapping the integration limits.



(a) Three-body (b) Four-body two-particles (c) Four-body three-particles

FIG. 5. Comparison between the analytical and MC generated invariant mass distributions of the three-body PS PDFs in (a) and the two possible four-body PS PDFs in (b),(c), respectively. Each of the PS PDFs are valid for trivial amplitudes and massless colliding and final state particles. The three-body PS PDFs appears in the three-body decay width (5.35) and the four-body cross section (6.30). The four-body PS PDFs appear in the four-body decay width (6.27) and the five-body cross section (7.22).

$$d^2\Gamma_3(m_{abc}) = \frac{|\mathcal{A}_4|^2}{16\pi m_{abc}^3}\,\eth\mathfrak{m}_{ab}^2\,\eth\mathfrak{m}_{bc}^2, \tag{5.34}$$

For massless final state particles the differential decay width with respect to $\mathfrak{m}_{ab}$ can be expressed as three-body PS probability distribution function (PDF)

$$\frac{1}{2\pi}\frac{\mathfrak{m}_{ab}}{\Gamma_3}\frac{d\Gamma_3}{d\mathfrak{m}_{ab}} = f_3^2\left(\frac{\mathfrak{m}_{ab}}{m_{abc}}\right), \qquad f_3^2(x) = 4x(1-x^2), \tag{5.35}$$

where the total decay width is

$$\Gamma_3(m_{abc}) = \frac{\lambda^2 m_{abc}}{(8\pi)^3}, \tag{5.36}$$

and we have used that due to the normalization (2.9)

$$\frac{\eth m^2}{dm} = \frac{m}{2\pi}. \tag{5.37}$$

A comparison with Monte Carlo (MC) data for the three-body PS PDF is presented in Fig. 5(a).

2. Two-particle scattering into two final particles

After inserting the differential three-body PS in either of the parametrizations (5.27) or (5.30) into the differential scattering cross section (2.14) of two particles with masses m_{abc} and m_c into two particles with masses m_a and m_b and integrating over the c.m. energy m_{ab} and the external Euler angle differential (5.26) it reads

$$d\sigma_3(m_{abc}, m_c; m_{ab}; m_a, m_b) = \frac{|\mathcal{A}_4|^2}{8\,V_2(m_{abc})}\frac{V_2(m_{ab})}{m_{ab}^2}\,\eth\cos\theta^a_{abc}(m_{ab}), \tag{5.38}$$

or alternatively

$$d\sigma_3(m_{abc}, m_c; m_{ab}; m_a, m_b) = \frac{|\mathcal{A}_4|^2}{16\,V_2^2(m_{abc})}\,\eth\mathfrak{m}_{bc}^2. \tag{5.39}$$

For the production via the trivial four scalar interaction (5.32) and in the limit of vanishing particle masses the total cross section for the c.m. energy m_{ab} is then

$$\sigma_3(m_{ab}) = \frac{\lambda^2}{16\pi m_{ab}^2}. \tag{5.40}$$

VI. FOUR-BODY INTERACTIONS

The invariant mass (2.5) of four particles is given by

$$m_{abcd}^2 = \mathfrak{m}_{abcd}^2 := \zeta \boldsymbol{p}_{abcd}^2, \qquad \boldsymbol{p}_{abcd} = \boldsymbol{p}_a + \boldsymbol{p}_b + \boldsymbol{p}_c + \boldsymbol{p}_d. \tag{6.1}$$

Besides four three-body constraints of the form (5.2) for the invariant masses $\mathfrak{m}_{abc}$, $\mathfrak{m}_{abd}$, $\mathfrak{m}_{acd}$, and $\mathfrak{m}_{bcd}$, which can be used to eliminate the noncanonical invariant masses $\mathfrak{m}_{ac}$, $\mathfrak{m}_{bd}$, $\mathfrak{m}_{acd}$, and $\mathfrak{m}_{abd}$, the four-body constraint can be expressed as

$$m_{abcd}^2 = \mathfrak{m}_{abc}^2 + \mathfrak{m}_{bcd}^2 + \mathfrak{m}_{ad}^2 - \mathfrak{m}_{bc}^2 - m_a^2 - m_d^2 \tag{6.2}$$

and can be used to eliminate the noncanonical invariant mass $\mathfrak{m}_{ad}$. The four-body PS is governed by a four-dimensional parallelotope $\square_4(m_{abcd}; m_a, m_b, m_c, m_d)$ which is triangulated in 12 different ways by pentatopes $\triangle_4(m_{abcd}; m_a, m_b, m_c, m_d)$.

A. Parallelotopes and pentatopes

The four-body Gram determinants (3.3) have mass-dimension six. The Gram determinant at the vertex $\kappa^a_{abcd}(\mathfrak{m}_{ab}, \mathfrak{m}_{abc})$ is given by

$$G_3^2(m_a, m_{abcd}; \mathfrak{m}_{ab}, \mathfrak{m}_{abc}) = \zeta G_3^2\begin{pmatrix} \boldsymbol{p}_a, \boldsymbol{p}_{ab}, \boldsymbol{p}_{abc} \\ \boldsymbol{p}_{abcd}, \boldsymbol{p}_{ab}, \boldsymbol{p}_{abc} \end{pmatrix}, \tag{6.3}$$

and a Laplace expansion in terms of minors (3.4) results in

$$\begin{aligned}\eta G_3^2(m_{abcd}, m_a; \mathfrak{m}_{ab}, \mathfrak{m}_{abc}) &= G_1^2(m_{abcd}, m_a) V_2^2(\mathfrak{m}_{ab}, \mathfrak{m}_{abc}) \\ &\quad - G_1^2(m_{abcd}, \mathfrak{m}_{ab}) G_2^2(m_a, \mathfrak{m}_{ab}; \mathfrak{m}_{abc}) - G_1^2(m_{abcd}, \mathfrak{m}_{abc}) G_2^2(m_a, \mathfrak{m}_{abc}; \mathfrak{m}_{ab}).\end{aligned} \tag{6.4}$$

The four-body CM determinant (3.6) reads

$$V_4^2(m_{abcd}; m_a, m_b, m_c, m_d) = \frac{1}{16}\begin{vmatrix} 0 & 1 & 1 & 1 & 1 & 1 \\ 1 & 0 & m_a^2 & \mathfrak{m}_{ab}^2 & \mathfrak{m}_{abc}^2 & m_{abcd}^2 \\ 1 & m_a^2 & 0 & m_b^2 & \mathfrak{m}_{bc}^2 & \mathfrak{m}_{bcd}^2 \\ 1 & \mathfrak{m}_{ab}^2 & m_b^2 & 0 & m_c^2 & \mathfrak{m}_{cd}^2 \\ 1 & \mathfrak{m}_{abc}^2 & \mathfrak{m}_{bc}^2 & m_c^2 & 0 & m_d^2 \\ 1 & m_{abcd}^2 & \mathfrak{m}_{bcd}^2 & \mathfrak{m}_{cd}^2 & m_d^2 & 0 \end{vmatrix}. \tag{6.5}$$

The volume of the four-dimensional parallelotope $\square_4(m_{abcd}; m_a, m_b, m_c, m_d)$ is then given by $V_4(m_{abcd}; m_a, m_b, m_c, m_d)$. The DJ determinant identity (3.18) allows one to express the volume compactly as

$$V_4^2(m_{abcd}; m_a, m_b, m_c, m_d) = -\frac{V_2^2(V_3(m_a, \mathfrak{m}_{bc}, m_d), V_3(m_b, \mathfrak{m}_{ac}, m_d), V_3(m_c, \mathfrak{m}_{ab}, m_d))}{V_2^2(m_d, \mathfrak{m}_{abc})}. \tag{6.6}$$

Limiting cases of the volume relevant for MST are

$$V_4^2 = \frac{1}{16}\begin{cases} 2\mathfrak{m}_{ab}^2\mathfrak{m}_{ac}^2\mathfrak{m}_{bd}^2\mathfrak{m}_{cd}^2 - \mathfrak{m}_{ab}^4\mathfrak{m}_{cd}^4 \\ +2\mathfrak{m}_{ac}^2\mathfrak{m}_{ad}^2\mathfrak{m}_{bc}^2\mathfrak{m}_{bd}^2 - \mathfrak{m}_{ac}^4\mathfrak{m}_{bd}^4 \\ +2\mathfrak{m}_{ab}^2\mathfrak{m}_{ad}^2\mathfrak{m}_{bc}^2\mathfrak{m}_{cd}^2 - \mathfrak{m}_{ad}^4 \end{cases} \quad \text{for } m_a = m_b = m_c = m_d = 0, \qquad \begin{cases} 0 \end{cases} \quad \text{for } m_a + m_b + m_c + m_d = m_{abcd}. \tag{6.7}$$

Hence the physical regime is determined by positive volumes. A Laplace expansion in terms of minors (3.13) results in

$$\begin{aligned}\eta V_4^2(m_{abcd}; m_a, m_b, m_c, m_d) &= m_a^2 V_3^2(m_b, m_c, m_d) - G_1^2(m_a, m_b) G_2^2(m_a, m_b; m_c, m_d) \\ &\quad - G_1^2(m_a, m_c) G_2^2(m_a, m_c; m_b, m_d) - G_1^2(m_a, m_d) G_2^2(m_a, m_d; m_b, m_c).\end{aligned} \tag{6.8}$$

B. Angle between decay planes

In the rest frame of the invariant mass $\mathfrak{m}_{ab}$ the cosine of the angle between two planes defined by the four involved momenta can be calculated to be

$$\cos\phi^a_{abcd}(\mathfrak{m}_{ab}, \mathfrak{m}_{abc}) := \frac{\mathsf{p}_a(\mathfrak{m}_{ab}) \times \mathsf{p}_{abc}(\mathfrak{m}_{ab})}{|\mathsf{p}_a(\mathfrak{m}_{ab}) \times \mathsf{p}_{abc}(\mathfrak{m}_{ab})|} \cdot \frac{\mathsf{p}_{abc}(\mathfrak{m}_{ab}) \times \mathsf{p}_{abcd}(\mathfrak{m}_{ab})}{|\mathsf{p}_{abc}(\mathfrak{m}_{ab}) \times \mathsf{p}_{abcd}(\mathfrak{m}_{ab})|}; \tag{6.9}$$

see also Fig. 2(a). It can be identified with the angle between the two tetrahedra $\triangle_3(m_a, \mathfrak{m}_{ab}, \mathfrak{m}_{abc})$ and $\triangle_3(m_{abcd}, \mathfrak{m}_{ab}, \mathfrak{m}_{abc})$ at the vertex $\kappa^a_{abcd}(\mathfrak{m}_{ab}, \mathfrak{m}_{abc})$ within the pentatope $\triangle_4(m_{abcd})$. Specifying the general equation for the cosine of such an angle (3.19) to the case of pentatopes results in the frame independent expression

$$\cos\phi^a_{abcd}(\mathfrak{m}_{ab}, \mathfrak{m}_{abc}) = \frac{G_3^2(m_a, m_{abcd}; \mathfrak{m}_{ab}, \mathfrak{m}_{abc})}{V_3(m_a, \mathfrak{m}_{ab}, \mathfrak{m}_{abc}) V_3(m_{abcd}, \mathfrak{m}_{ab}, \mathfrak{m}_{abc})}. \tag{6.10}$$

Note that this expression is not only invariant under exchange of m_a and m_{abcd} but also under exchange of $\mathfrak{m}_{ab}$ and $\mathfrak{m}_{abc}$. Using the Laplace expansion (6.4) this equation can be solved for the invariant mass

$$\mathfrak{m}^2_{bcd} = m^2_{abcd} + m^2_a - 2\frac{g^a_{abcd}(\mathfrak{m}_{ab}, \mathfrak{m}_{abc})}{V_2^2(\mathfrak{m}_{ab}, \mathfrak{m}_{abc})}, \tag{6.11}$$

where

$$\begin{aligned} g^a_{abcd}(\mathfrak{m}_{ab}, \mathfrak{m}_{abc}) = {} & \eta V_3(m_a, m_b, m_c) V_3(\mathfrak{m}_{ab}, m_c, m_d) \cos\phi^a_{abcd}(\mathfrak{m}_{ab}, \mathfrak{m}_{abc}) \\ & + G_1^2(m_a, \mathfrak{m}_{ab}) G_2^2(m_{abcd}, \mathfrak{m}_{ab}; \mathfrak{m}_{abc}) + G_1^2(m_a, \mathfrak{m}_{abc}) G_2^2(m_{abcd}, \mathfrak{m}_{abc}; \mathfrak{m}_{ab}). \end{aligned} \tag{6.12}$$

The volumes of the tetrahedra appearing here can be expressed in terms of polar opening angles using (5.19) and the derivative of the invariant mass square $\mathfrak{m}^2_{bcd}$ with respect to the cosine of the azimuthal decay plane angle reads

$$\frac{d\mathfrak{m}^2_{bcd}}{d\cos\phi^a_{abcd}(\mathfrak{m}_{ab}, \mathfrak{m}_{abc})} = -2\eta \frac{V_3(m_a, \mathfrak{m}_{ab}, \mathfrak{m}_{abc}) V_3(m_{abcd}, \mathfrak{m}_{ab}, \mathfrak{m}_{abc})}{V_2^2(\mathfrak{m}_{ab}, \mathfrak{m}_{abc})}. \tag{6.13}$$

Specifying the general equation for the sine of the angle between two simplices (3.20) to the case of pentatopes results in

$$\sin\phi^a_{abcd}(\mathfrak{m}_{ab}, \mathfrak{m}_{abc}) = \frac{V_2(\mathfrak{m}_{ab}, \mathfrak{m}_{abc}) V_4(m_a, m_b, m_c, m_d)}{V_3(m_a, \mathfrak{m}_{ab}, \mathfrak{m}_{abc}) V_3(m_{abcd}, \mathfrak{m}_{ab}, \mathfrak{m}_{abc})}. \tag{6.14}$$

Therefore, using the differential of the invariant mass with respect to the cosine (6.13) the differential of the invariant mass with respect to the azimuthal decay plane angle reads

$$\frac{d\mathfrak{m}^2_{bcd}}{d\phi^a_{abcd}(\mathfrak{m}_{ab}, \mathfrak{m}_{abc})} = 2\eta \frac{V_4(m_{abcd}; m_a, m_b, m_c, m_d)}{V_2(\mathfrak{m}_{ab}, \mathfrak{m}_{abc})}. \tag{6.15}$$

The tangent

$$\tan\phi^a_{abcd}(\mathfrak{m}_{ab}, \mathfrak{m}_{abc}) = \frac{V_2(\mathfrak{m}_{ab}, \mathfrak{m}_{abc}) V_4(m_a, m_b, m_c, m_d)}{G_3^2(m_a, m_{abcd}; \mathfrak{m}_{ab}, \mathfrak{m}_{abc})} \tag{6.16}$$

allows one to express the volume without depending on three-dimensional volumes.

C. Invariant angle differentials

Using the differential relations (5.17) and (6.15) the solid angle differential (4.28) can be parametrized using invariant quantities [9]

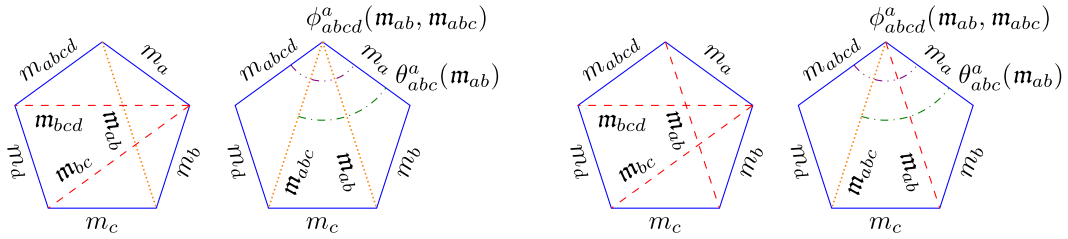
$$\eth^2\Omega^a_{abcd}(\mathfrak{m}_{abc}; \mathfrak{m}_{ab}) = \frac{\mathfrak{m}^2_{ab}}{2\,V_2(\mathfrak{m}_{ab})} \frac{\eth\mathfrak{m}^2_{bc}\,\eth\mathfrak{m}^2_{bcd}}{V_4(m_{abcd})}. \tag{6.17}$$

[9]Where we have taken into account that the invariant description of the decay plane angle (6.14) is constrained to have half the domain (3.21) of the azimuthal angle (4.30).

Additionally, using the differential two-body PS (4.36) together with this expressions allows one to parametrize the augmented two-body PS differential (2.11) in terms of invariants

$$d^3\Phi'_2(m_{ab}; m_c, m_d) = \frac{\eth\mathfrak{m}^2_{ab}\,\eth\mathfrak{m}^2_{bc}\,\eth\mathfrak{m}^2_{bcd}}{V_4(m_{abcd})}. \tag{6.18}$$

The comparison of the two parametrizations of these differentials in Fig. 6 as well as the appearance of the four-dimensional volume illustrates that these differentials are connected to the four-body PS. Furthermore, the Euler angle differential (5.25) can be invariantly parametrized using the differential relation (6.15) together with the invariant parametrization of the solid angle differential (6.17)



(a) $\eth^2\Omega^a_{abcd}(m_{abc}; m_{ab})$ (b) $d^3\Phi'_2(m_{ab}; m_c, m_d)$

FIG. 6. Comparison between the invariant mass and the angular parametrization of the solid angle differential in (a) as well as the augmented two-body PS differential in (b). For the solid angle differential the invariant mass parametrization is given in (6.17) and the angular parametrization is given in (4.28). For the augmented two-body PS differential the invariant mass parametrization is given in (6.18) and the angular parametrization is given in (2.11). Particle masses are presented as solid blue lines, invariant masses appearing in the differential as dashed red lines, further invariant masses as dotted orange lines, polar angles as dash-dotted green arc, and azimuthal angles as dash-dot-dotted purple arcs. The relation between the invariant description of the solid angle differential and frame dependent depictions is discussed in Fig. 2.

$$\eth^3\Omega^{a;ab}_{abcde;abcd}(m_{abc}) = \frac{m^2_{abc}}{2\,V_4(m_{abcd})}\frac{\eth m^2_{bcd}\,\eth m^2_{cd}\,\eth m^2_{cde}}{V_4(m_{bcde})}. \tag{6.19}$$

The comparison of the two parametrizations in Fig. 7 show that this differential is connected to the five-body PS discussed in Sec. VII C.

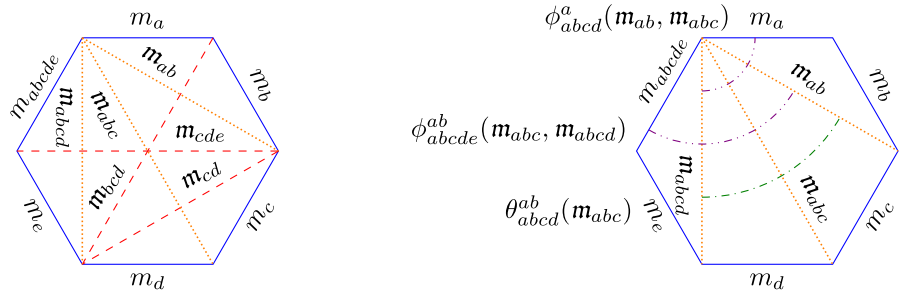
D. Four-body phase space

Using the recursion relation (2.8), the differential four-body PS can be expressed as a function of a differential three-body PS (5.30) together with an augmented two-body PS differential (2.11)

$$d^8\Phi_4(m_{abcd}; m_e, m_f) = d^5\Phi_3(m_{abcd}; \mathfrak{m}_{ab}, m_c, m_d; m_e, m_f) \times d^3\Phi'_2(\mathfrak{m}_{ab}; m_c, m_d), \tag{6.20}$$

using the invariant parametrization for the differential three-body PS (5.30) and the augmented two-body PS differential (6.18) the differential four-body PS reads

$$d^8\Phi_4(m_{abcd}; m_e, m_f) = \eth m^2_{abc}\,\eth m^2_{cd}\frac{\eth m^2_{ab}\,\eth m^2_{bc}\,\eth m^2_{bcd}}{V_4(m_{abcd})}\,\eth^3\Omega^{ab;abc}_{abcdef;abcde}(m_{abcd}), \tag{6.21}$$



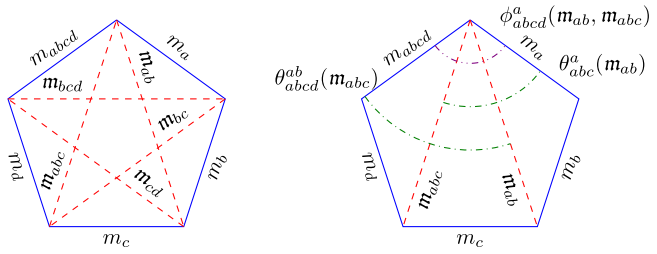
(a) Invariant mass parametrization (b) Angular parametrization

FIG. 7. Comparison between the invariant mass and the angular parametrization of the Euler angle differential in (a),(b), respectively. The Euler angle differential in the invariant mass parametrization is given in (6.19) and in the angular parametrization in (5.25). Particle masses are presented as solid blue lines, invariant masses appearing in the differential as dashed red lines, further invariant masses as dotted orange lines, polar angles as dash-dotted green arc, and azimuthal angles as dash-dot-dotted purple arcs.

Therefore, the four-body PS parametrized by invariant masses is inversely proportional to the volume of a four-dimensional parallelotope. This parametrization is depicted in Fig. 8(a). The explicit appearance of the volume and the nontrivial integration limits of the form (5.9) can become problematic for analytic calculations [10,14]. Alternatively, the differential four-body PS can be constructed from three two-body PSs

$$\begin{aligned} d^8\Phi_4(m_{abcd};m_e,m_f) &= d^2\Phi_2(m_{abcd};\mathfrak{m}_{abc},m_d;m_e,m_f) \\ &\times d^3\Phi_2'(\mathfrak{m}_{abc};\mathfrak{m}_{ab},m_c;m_d,m_e) \\ &\times d^3\Phi_2'(\mathfrak{m}_{ab};m_c,m_d). \end{aligned} \tag{6.22}$$

Using the explicit expressions for the augmented two-body PS differential (2.11) and the differential two-body PS (4.36), the four-body PS reads



(a) Invariant masses (b) Angular variables

FIG. 8. Diagrams of the four-body PS parametrized using invariant masses (6.21) in (a) and angular variables (6.23) in (b).

$$\begin{aligned} d^8\Phi_4(m_{abcd};m_e,m_f) = 4\,V_2(m_{abcd})\frac{V_2(\mathfrak{m}_{abc})}{\mathfrak{m}_{abc}^2}\frac{V_2(\mathfrak{m}_{ab})}{\mathfrak{m}_{ab}^2}\,\eth\mathfrak{m}_{abc}^2\,\eth\mathfrak{m}_{ab}^2 \\ \eth\cos\theta^{ab}_{abcd}(\mathfrak{m}_{abc})\,\eth\phi^a_{abcd}(\mathfrak{m}_{abc},\mathfrak{m}_{ab})\,\eth\cos\theta^a_{abc}(\mathfrak{m}_{ab})\,\eth^3\Omega^{ab;abc}_{abcdef;abcde}(m_{abcd}), \end{aligned} \tag{6.23}$$

This parametrization is depicted in Fig. 8(b). However, further parametrizations have also been studied [41].

E. Four-body processes

In the following we use a trivial interaction between five scalar particles with Lagrangian and amplitude

$$\mathcal{L}_5 \supset \frac{1}{5!\Lambda}\phi_{abcd}\phi_a\phi_b\phi_c\phi_d, \qquad \mathcal{A}_5 = \frac{\mathrm{i}}{\Lambda}, \tag{6.24}$$

in the limit of massless colliding and final state particles.

1. Decays into three final particles

The partial decay width (2.13) into four final state particles via the trivial interaction (6.24) in the rest frame of the decaying particle using the PS parametrization (6.23) reads after integration over the external Euler angle differential

$$\begin{aligned} d^5\Gamma_4(m_{abcd}) = \frac{|\mathcal{A}_5|^2}{4\pi}\frac{V_2(m_{abcd})}{m_{abcd}^3}\frac{V_2(\mathfrak{m}_{abc})}{\mathfrak{m}_{abc}^2}\frac{V_2(\mathfrak{m}_{ab})}{\mathfrak{m}_{ab}^2}\,\eth\mathfrak{m}_{abc}^2\,\eth\mathfrak{m}_{ab}^2 \\ \eth\cos\theta^{ab}_{abcd}(\mathfrak{m}_{abc})\,\eth\phi^a_{abcd}(\mathfrak{m}_{abc},\mathfrak{m}_{ab})\,\eth\cos\theta^a_{abc}(\mathfrak{m}_{ab}). \end{aligned} \tag{6.25}$$

After evaluating four integrals the one-dimensional differential decay widths with respect to the invariant masses $\mathfrak{m}_{ab}$ and $\mathfrak{m}_{abc}$ read

$$\frac{1}{2\pi}\frac{\mathfrak{m}_{ab}}{\Gamma_4}\frac{d\Gamma_4}{d\mathfrak{m}_{ab}} = f_4^2\left(\frac{\mathfrak{m}_{ab}}{m_{abcd}}\right), \qquad \frac{1}{2\pi}\frac{\mathfrak{m}_{abc}}{\Gamma_4}\frac{d\Gamma_4}{d\mathfrak{m}_{abc}} = f_4^3\left(\frac{\mathfrak{m}_{abc}}{m_{abcd}}\right), \tag{6.26}$$

where we have used the derivative (5.37). The four-body PS PDF for massless final state particles appearing here are

$$f_4^2(x) = 12x(1-x^4+2x^2\ln x^2), \qquad f_4^3(x) = 12x^3(1-x^2), \tag{6.27}$$

and the total decay width is

$$\Gamma_4(m_{abcd}) = \frac{2m_{abcd}^3}{3(8\pi)^5\Lambda^2}. \tag{6.28}$$

A comparison with MC data is shown in Figs. 5(b) and 5(c), respectively.

2. Two particle scattering into three final particles

The differential production cross section (2.14) of the four-body process (6.24) in the parametrization (6.23) reads after integration over the c.m. energy and the external Euler angle differential (5.26)

$$d^7\sigma_4(m_{abcd}, m_d; m_{abc}) = \frac{|\mathcal{A}_5|^2}{4\,V_2(m_{abcd})}\frac{V_2(m_{abc})}{m_{abc}^2}\frac{V_2(\mathfrak{m}_{ab})}{\mathfrak{m}_{ab}^2}\,\eth\mathfrak{m}_{ab}^2 \\ \eth\cos\theta^{ab}_{abcd}(m_{abc})\,\eth\phi^{a}_{abcd}(m_{abc},\mathfrak{m}_{ab})\,\eth\cos\theta^{a}_{abc}(\mathfrak{m}_{ab}), \tag{6.29}$$

Hence in the limit of vanishing particle masses the distribution of the differential production cross section is given by the three-body PS PDF (5.35)

$$\frac{1}{2\pi}\frac{\mathfrak{m}_{ab}}{\sigma_4}\frac{d\sigma_4}{d\mathfrak{m}_{ab}} = f_3^2\left(\frac{\mathfrak{m}_{ab}}{m_{abc}}\right), \tag{6.30}$$

where the total production cross section

$$\sigma_4 = \frac{1}{(8\pi)^3\Lambda^2} \tag{6.31}$$

is independent of the c.m. energy. A comparison with the MC generated data is presented in Fig. 5(a).

VII. FIVE-BODY INTERACTIONS

The invariant mass (2.5) of five particles is given by

$$m_{abcde}^2 = \mathfrak{m}_{abcde}^2 \coloneqq \zeta \boldsymbol{p}_{abcde}^2, \\ \boldsymbol{p}_{abcde} = \boldsymbol{p}_a + \boldsymbol{p}_b + \boldsymbol{p}_c + \boldsymbol{p}_d + \boldsymbol{p}_e. \tag{7.1}$$

Besides the three-body constraints of the form (5.2) and the four-body constraints of the form (6.2) the five-body constraint can be expressed as

$$m_{abcde}^2 = \mathfrak{m}_{abcd}^2 + \mathfrak{m}_{bcde}^2 + \mathfrak{m}_{ae}^2 - \mathfrak{m}_{bcd}^2 - m_a^2 - m_e^2, \tag{7.2}$$

and can be used to eliminate the noncanonical invariant mass $\mathfrak{m}_{ae}$.

A. Parallelotopes and five-simplex

The five-body Gram determinants (3.3) have mass-dimension eight. The Gram determinant at the vertex $\kappa^a_{abcde}(\mathfrak{m}_{ab}, \mathfrak{m}_{abc}, \mathfrak{m}_{abcd})$ is given by

$$G_4^2(m_a, m_{abcde}; \mathfrak{m}_{ab}, \mathfrak{m}_{abc}, \mathfrak{m}_{abcd}) \\ = G_4^2\begin{pmatrix} \boldsymbol{p}_a, \boldsymbol{p}_{ab}, \boldsymbol{p}_{abc}, \boldsymbol{p}_{abcd} \\ \boldsymbol{p}_{abcde}, \boldsymbol{p}_{ab}, \boldsymbol{p}_{abc}, \boldsymbol{p}_{abcd} \end{pmatrix}, \tag{7.3}$$

and a Laplace expansion in terms of minors (3.4) results in

$$\eta G_4^2(m_{abcde}, m_a; \mathfrak{m}_{ab}, \mathfrak{m}_{abc}, \mathfrak{m}_{abcd}) = G_1^2(m_{abcde}, m_a)V_3^2(\mathfrak{m}_{ab}, \mathfrak{m}_{abc}, \mathfrak{m}_{abcd}) \\ - G_1^2(m_{abcde}, \mathfrak{m}_{ab})G_3^2(m_a, \mathfrak{m}_{ab}; \mathfrak{m}_{abc}, \mathfrak{m}_{abcd}) \\ - G_1^2(m_{abcde}, \mathfrak{m}_{abc})G_3^2(m_a, \mathfrak{m}_{abc}; \mathfrak{m}_{ab}, \mathfrak{m}_{abcd}) \\ - G_1^2(m_{abcde}, \mathfrak{m}_{abcd})G_3^2(m_a, \mathfrak{m}_{abcd}; \mathfrak{m}_{ab}, \mathfrak{m}_{abc}). \tag{7.4}$$

The five-body CM determinant (3.6) is

$$V_5^2(m_{abcde}; m_a, m_b, m_c, m_d, m_e) = \frac{1}{32}\begin{vmatrix} 0 & 1 & 1 & 1 & 1 & 1 & 1 \\ 1 & 0 & m_a^2 & \mathfrak{m}_{ab}^2 & \mathfrak{m}_{abc}^2 & \mathfrak{m}_{abcd}^2 & m_{abcde}^2 \\ 1 & m_a^2 & 0 & m_b^2 & \mathfrak{m}_{bc}^2 & \mathfrak{m}_{bcd}^2 & \mathfrak{m}_{bcde}^2 \\ 1 & \mathfrak{m}_{ab}^2 & m_b^2 & 0 & m_c^2 & \mathfrak{m}_{cd}^2 & \mathfrak{m}_{cde}^2 \\ 1 & \mathfrak{m}_{abc}^2 & \mathfrak{m}_{bc}^2 & m_c^2 & 0 & m_d^2 & \mathfrak{m}_{de}^2 \\ 1 & \mathfrak{m}_{abcd}^2 & \mathfrak{m}_{bcd}^2 & \mathfrak{m}_{cd}^2 & m_d^2 & 0 & m_e^2 \\ 1 & m_{abcde}^2 & \mathfrak{m}_{bcde}^2 & \mathfrak{m}_{cde}^2 & \mathfrak{m}_{de}^2 & m_e^2 & 0 \end{vmatrix}. \tag{7.5}$$

Therefore, the five-dimensional parallelotope is parametrized by nine canonical invariant masses.

B. Angle and constraint

Specifying the general equation for the cosine of an angle (3.19) to five dimensions results in

$$\cos\psi^{a}_{abcde}(\mathfrak{m}_{ab},\mathfrak{m}_{abc},\mathfrak{m}_{abcd}) = \frac{G_4^2(m_a, m_{abcd};\mathfrak{m}_{ab},\mathfrak{m}_{abc},\mathfrak{m}_{abcd})}{V_4(m_a,\mathfrak{m}_{ab},\mathfrak{m}_{abc},\mathfrak{m}_{abcd})V_4(m_{abcde},\mathfrak{m}_{ab},\mathfrak{m}_{abc},\mathfrak{m}_{abcd})}, \tag{7.6}$$

and similarly, the sine (3.20) reads

$$\sin\psi^{a}_{abcde}(\mathfrak{m}_{ab},\mathfrak{m}_{abc},\mathfrak{m}_{abcd}) = \frac{V_3(\mathfrak{m}_{ab},\mathfrak{m}_{abc},\mathfrak{m}_{abcd})V_5(m_{abcde})}{V_4(m_a,\mathfrak{m}_{ab},\mathfrak{m}_{abc},\mathfrak{m}_{abcd})V_4(m_{abcde},\mathfrak{m}_{ab},\mathfrak{m}_{abc},\mathfrak{m}_{abcd})}. \tag{7.7}$$

Since the five-dimensional volume (7.5) must vanish in a four-dimensional MST [8] only eight of the nine canonical invariant masses are independent; see also the discussion in Sec. III B. Therefore, we require that

$$G_4^2(m_a, m_{abcde};\mathfrak{m}_{ab},\mathfrak{m}_{abc},\mathfrak{m}_{abcd}) = V_4(m_a,\mathfrak{m}_{ab},\mathfrak{m}_{abc},\mathfrak{m}_{abcd})V_4(m_{abcde},\mathfrak{m}_{ab},\mathfrak{m}_{abc},\mathfrak{m}_{abcd}). \tag{7.8}$$

Using the Laplace expansion (7.4) to solve this expression for the invariant mass $\mathfrak{m}_{bcde}$ results in the constraint

$$\mathfrak{m}^2_{bcde} = m_a^2 + m^2_{abcde} - 2\frac{g^{a}_{abcde}(\mathfrak{m}_{ab},\mathfrak{m}_{abc},\mathfrak{m}_{abcd})}{V_3^2(\mathfrak{m}_{ab},\mathfrak{m}_{abc},\mathfrak{m}_{abcd})}, \tag{7.9}$$

where

$$\begin{aligned} g^{a}_{abcde}(\mathfrak{m}_{ab},\mathfrak{m}_{abc},\mathfrak{m}_{abcd}) = {}& \eta V_4(m_a,\mathfrak{m}_{ab},\mathfrak{m}_{abc},\mathfrak{m}_{abcd})V_4(m_{abcde},\mathfrak{m}_{ab},\mathfrak{m}_{abc},\mathfrak{m}_{abcd}) \\ & + G_1^2(m_{abcde},\mathfrak{m}_{ab})G_3^2(m_a,\mathfrak{m}_{ab};\mathfrak{m}_{abc},\mathfrak{m}_{abcd}) \\ & + G_1^2(m_{abcde},\mathfrak{m}_{abc})G_3^2(m_a,\mathfrak{m}_{abc};\mathfrak{m}_{ab},\mathfrak{m}_{abcd}) \\ & + G_1^2(m_{abcde},\mathfrak{m}_{abcd})G_3^2(m_a,\mathfrak{m}_{abcd};\mathfrak{m}_{ab},\mathfrak{m}_{abc}). \end{aligned} \tag{7.10}$$

The volumes V_3 and V_4 can be expressed in terms of polar opening angles (5.19) and azimuthal decay plane angles (6.16), respectively. This constraint allows one to eliminate the invariant mass $\mathfrak{m}_{bcde}$.

C. Five-body phase space

The differential five-body PS can be constructed from a differential three-body PS (5.23) together with two augmented two-body PS differentials (2.11) using the recursion relation (2.8)

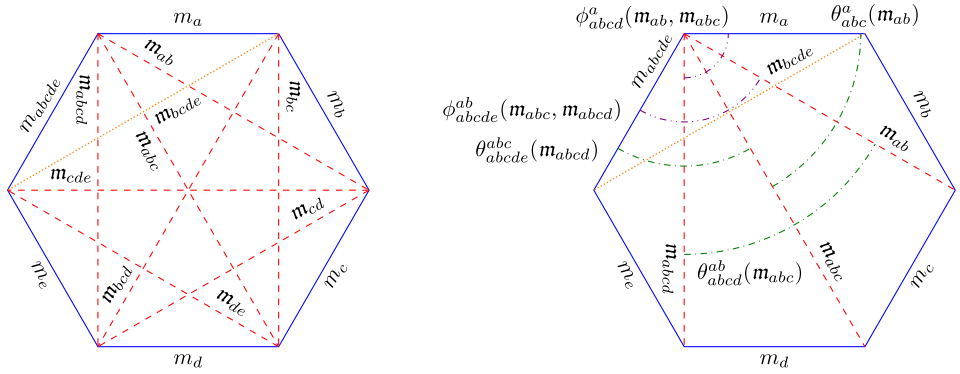
$$d^{11}\Phi_5(m_{abcde};m_f,m_g) = d^5\Phi_3(\mathfrak{m}_{abcde};m_{abc},m_d,m_e;m_f,m_g)d^3\Phi_2'(\mathfrak{m}_{abc};\mathfrak{m}_{ab},m_c;m_d,m_e)d^3\Phi_2'(\mathfrak{m}_{ab};m_c,m_d). \tag{7.11}$$

After inserting the invariant parametrizations of the differential three-body PS (5.30) and the invariant expression for the augmented two-body PS differential (6.18) and integrating over the external Euler angle differential (5.26) the differential five-body PS

$$d^8\Phi_5(m_{abcde}) = \frac{1}{8\pi}\,\text{đ}\mathfrak{m}^2_{abcd}\,\text{đ}\mathfrak{m}^2_{de}\frac{\text{đ}m^2_{abc}\,\text{đ}m^2_{cd}\,\text{đ}m^2_{cde}}{V_4(\mathfrak{m}_{bcde})}\frac{\text{đ}m^2_{ab}\,\text{đ}m^2_{bc}\,\text{đ}m^2_{bcd}}{V_4(\mathfrak{m}_{abcd})}, \tag{7.12}$$

depends only on invariant masses. The diagram of the five-body PS in this parametrization is shown in Fig. 9(a). The appearance of four-dimensional volumes (6.5) and nontrivial integration limits (5.9) renders this parametrization impractical for analytical calculations. Alternatively, the differential five-body PS can be constructed from four differential two-body PSs

$$\begin{aligned} d^{11}\Phi_5(m_{abcde};m_f,m_g) = {}& d^2\Phi_2(m_{abcde};\mathfrak{m}_{abcd},m_e;m_f,m_g) \\ & \times d^3\Phi_2'(\mathfrak{m}_{abcd};\mathfrak{m}_{abc},m_d;m_e,m_f)d^3\Phi_2'(\mathfrak{m}_{abc};\mathfrak{m}_{ab},m_c;m_d,m_e)d^3\Phi_2'(\mathfrak{m}_{ab};m_c,m_d). \end{aligned} \tag{7.13}$$



(a) Invariant masses (b) Angular variables

FIG. 9. Diagrams of the five-body PS parametrized using invariant masses (7.12) in (a) and angular variables (7.14) in (b). While the parallelotope is parametrized by nine variables the PS in MST is constrained since the five-dimensional volume (7.5) must vanish. Therefore one of the invariant masses (dotted orange line) can be eliminated using the constraint (7.9).

After inserting the explicit expressions for the augmented two-body PS differential (2.11) and the differential two-body PS (4.36) and integrating over the external Euler angle differential (5.26) the differential five-body PS reads

$$\begin{aligned} d^8\Phi_5(m_{abcde}) = \frac{V_2(m_{abcde})}{\pi}\frac{V_2(m_{abcd})}{m^2_{abcd}}\frac{V_2(m_{abc})}{m^2_{abc}}\frac{V_2(m_{ab})}{m^2_{ab}}\,\mathrm{d}m^2_{abcd}\,\mathrm{d}m^2_{abc}\,\mathrm{d}m^2_{ab} \\ \mathrm{d}\cos\theta^{abc}_{abcde}(m_{abcd})\,\mathrm{d}\phi^{ab}_{abcde}(m_{abcd}, m_{abc})\,\mathrm{d}\cos\theta^{ab}_{abcd}(m_{abc}) \\ \mathrm{d}\phi^{a}_{abcd}(m_{abc}, m_{ab})\,\mathrm{d}\cos\theta^{a}_{abc}(m_{ab}). \end{aligned} \tag{7.14}$$

The PS diagram of this parametrization is shown in Fig. 9(b).

D. Five-body processes

In the following we work with the trivial interaction of six scalar particles with Lagrangian and amplitude

$$\mathcal{L}_6 \supset \frac{1}{6!\Lambda^2}\phi_{abcde}\phi_a\phi_b\phi_c\phi_d\phi_e, \qquad \mathcal{A}_6 = \frac{\mathrm{i}}{\Lambda^2} \tag{7.15}$$

and massless colliding and final state particles.

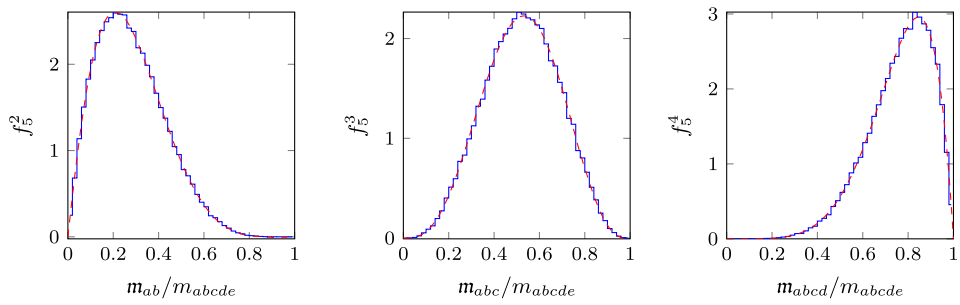
1. Decays into five final particles

The differential decay width (2.13) using the parametrization (7.14) of the differential five-body PS reads after integrating over the external Euler angle differential (5.26)

$$\begin{aligned} d^8\Gamma_5(m_{abcde}) = \frac{|\mathcal{A}_6|^2}{2\pi}\frac{V_2(m_{abcde})}{m^3_{abcde}}\frac{V_2(m_{abcd})}{m^2_{abcd}}\frac{V_2(m_{abc})}{m^2_{abc}}\frac{V_2(m_{ab})}{m^2_{ab}}\,\mathrm{d}m^2_{abcd}\,\mathrm{d}m^2_{abc}\,\mathrm{d}m^2_{ab} \\ \mathrm{d}\cos\theta^{abc}_{abcde}(m_{abcd})\,\mathrm{d}\phi^{ab}_{abcde}(m_{abcd}, m_{abc})\,\mathrm{d}\cos\theta^{ab}_{abcd}(m_{abc}) \\ \mathrm{d}\phi^{a}_{abcd}(m_{abc}, m_{ab})\,\mathrm{d}\cos\theta^{a}_{abc}(m_{ab}). \end{aligned} \tag{7.16}$$

The distribution of the one-dimensional differential decay width with respect to the invariant masses $\mathfrak{m}_{ab}$, $\mathfrak{m}_{abc}$, and $\mathfrak{m}_{abcd}$ are

$$\frac{1}{2\pi}\frac{\mathfrak{m}_{ab}}{\Gamma_5}\frac{d\Gamma_5}{d\mathfrak{m}_{ab}} = f^2_5\left(\frac{\mathfrak{m}_{ab}}{m_{abcde}}\right), \qquad \frac{1}{2\pi}\frac{\mathfrak{m}_{abc}}{\Gamma_5}\frac{d\Gamma_5}{d\mathfrak{m}_{abc}} = f^3_5\left(\frac{\mathfrak{m}_{abc}}{m_{abcde}}\right), \tag{7.17a}$$



(a) Two particles (b) Three particles (c) Four particles

FIG. 10. Comparison between the analytical and MC generated five-body PS PDFs for massless final state particles (7.18) and for invariant masses of two, three, and four particle in (a),(b),(c), respectively. These PDFs appear in the five-body decay width (7.17) and the six-body cross section.

$$\frac{1}{2\pi}\frac{\mathfrak{m}_{abcd}}{\Gamma_5}\frac{d\Gamma_5}{d\mathfrak{m}_{abcd}} = f_5^4\left(\frac{\mathfrak{m}_{abcd}}{m_{abcde}}\right), \tag{7.17b}$$

where the five-body PS PDFs for massless final state particles are

$$f_5^2(x) = 24x^5(1-x^2), \quad f_5^3(x) = 72x^3(1-x^4+2x^2\ln x^2), \tag{7.18a}$$

$$f_5^4(x) = 24x[1+9(x^2-x^4)-x^6+6(x^2+x^4)\ln x^2], \tag{7.18b}$$

and the total decay width is

$$\Gamma_5(m_{abcde}) = \frac{2m_{abcde}^5}{3^2(8\pi)^7\Lambda^4}. \tag{7.19}$$

A comparison with MC data is presented in Fig. 10.

2. Two-particle scattering into four final particles

After inserting the parametrization (7.14) of the differential five-body PS into the differential production cross section (2.14) and integrating over the external Euler angle differential (5.26) and the c.m. energy m_{abcd} it reads

$$\begin{aligned} d^7\sigma_5(m_{abcde}, m_e; m_{abcd}) = {} & \frac{|\mathcal{A}_6|^2}{2\,V_2(m_{abcde})}\frac{V_2(m_{abcd})}{m_{abcd}^2}\frac{V_2(\mathfrak{m}_{abc})}{\mathfrak{m}_{abc}^2}\frac{V_2(\mathfrak{m}_{ab})}{\mathfrak{m}_{ab}^2}\,đ\mathfrak{m}_{abc}^2\,đ\mathfrak{m}_{ab}^2 \\ & đ\cos\theta_{abcde}^{abc}(m_{abcd})\,đ\phi_{abcde}^{ab}(\mathfrak{m}_{abcd}, m_{abc})\,đ\cos\theta_{abcd}^{ab}(\mathfrak{m}_{abc}) \\ & đ\phi_{abcd}^{a}(\mathfrak{m}_{abc}, \mathfrak{m}_{ab})\,đ\cos\theta_{abc}^{a}(\mathfrak{m}_{ab}), \end{aligned} \tag{7.20}$$

The total production cross section for the trivial amplitude (7.15) and massless initial and final state particles is then

$$\sigma_5(m_{abcde}) = \frac{2m_{abcd}^2}{3(8\pi)^5\Lambda^4}. \tag{7.21}$$

The two- and three-particle distributions of the one-dimensional differential cross section are

$$\frac{1}{2\pi}\frac{\mathfrak{m}_{ab}}{\sigma_5}\frac{d\sigma_5}{d\mathfrak{m}_{ab}} = f_4^2\left(\frac{\mathfrak{m}_{ab}}{m_{abcd}}\right), \qquad \frac{1}{2\pi}\frac{\mathfrak{m}_{abc}}{\sigma_5}\frac{d\sigma_5}{d\mathfrak{m}_{abc}} = f_4^3\left(\frac{\mathfrak{m}_{abc}}{m_{abcd}}\right), \tag{7.22}$$

where the four-body PS PDFs are given in (6.27). A comparison with MC data is shown in Figs. 5(b) and 5(c).

VIII. MULTIBODY INTERACTIONS

The volume of the parallelotope that governs an n-body interaction (3.6) can be parametrized by $(n-2)(n+1)/2$ canonical invariant masses. Since volumes with dimensions larger than four have to vanish [8], $(n-4)(n-3)/2$ constraints of the form (7.9) have to be considered for $n > 2$. Therefore the differential n-dimensional PS is parametrized by $3n-7$ independent internal degrees of freedom.

A. Phase space

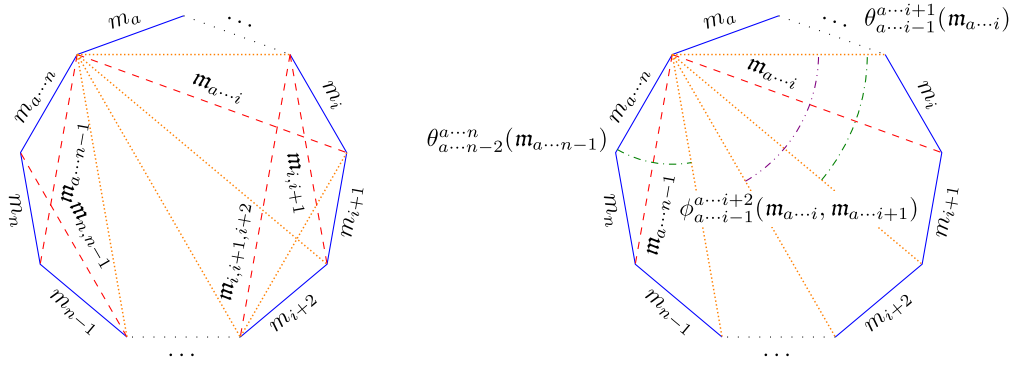
Using the recursion relation (2.8) repeatedly the differential n-body PS can be written in terms of a differential three-body PS (5.23) and a product of augmented two-body PS differentials (2.11)

$$d^{3n-4}\Phi_n(m_{a\cdots n};m_{n+1},\ldots)=d^5\Phi_3(m_{a\cdots n};\mathfrak{m}_{a\cdots n-2},m_{n-1},m_n;m_{n+1},\ldots)\prod_{i=b}^{n-2}d^3\Phi_2'(\mathfrak{m}_{a\cdots i};m_{i+1},m_{i+2}). \tag{8.1}$$

After using the invariant expressions for the differential three-body PS (5.30) as well as for the augmented two-body PS differentials (6.18) and integrating over the external Euler angle differential (5.26) the invariant expression for the differential n-body PS reads [11]

$$d^{3n-7}\Phi_n(m_{a\cdots n})=\frac{1}{8\pi}\,\text{đ}\mathfrak{m}^2_{a\cdots n-1}\,\text{đ}\mathfrak{m}^2_{n,n-1}\prod_{i=b}^{n-2}\frac{\text{đ}\mathfrak{m}^2_{a\cdots i}\,\text{đ}\mathfrak{m}^2_{i,i+1}\,\text{đ}\mathfrak{m}^2_{i,i+1,i+2}}{V_4(\mathfrak{m}_{a\cdots i-1},m_i,m_{i+1},m_{i+2})}, \tag{8.2}$$

The diagram of the differential n-body PS in this parametrization is presented in Fig. 11(a). In particular this expression recovers the frame independent parametrization for the differential three-body PS (5.30), the differential four-body PS (6.21), and the differential five-body PS (7.12). While this expression depends only on integrals over squares of invariant masses, the appearance of four-dimensional volumes (6.5) and nontrivial integration limits of the type (5.9) render the expression impractical for analytical calculations. The advantages and disadvantages of a purely invariant description as well as the ordering of the integration limits for numerical calculations is an active field of research [25,42,43].



(a) Invariant masses (b) Angular variables

FIG. 11. Diagrams of the n-body PS when parametrized using invariant masses (8.2) in (a) and angular variables (8.4) in (b). The on-shell masses of the final state particles are shown as solid blue lines, the integrals over invariant masses as dashed red lines, further invariant masses as dotted orange lines, polar opening angles as dashed-dotted green arcs, and azimuthal decay-plane angles as dashed-double-dotted purple arcs. Both depictions show that $n-3$ different four-body PSs, spanned by variables labeled with an i are involved, while the last two external particles span a three-body PS that contains variables labeled with an n. See Figs. 1 and 4 for a depiction of these simple PSs.

Alternatively, the differential n-body PS (8.1) can be rewritten in terms of a differential two-body PS and a product of augmented two-body PS differentials

$$d^{3n-4}\Phi_n(m_{a\cdots n};m_{n+1},\ldots)=d^2\Phi_2(m_{a\cdots n};\mathfrak{m}_{a\cdots n-1},m_n;m_{n+1},\ldots)\prod_{i=b}^{n-1}d^3\Phi_2'(\mathfrak{m}_{a\cdots i};m_{i+1},m_{i+2}). \tag{8.3}$$

Using the explicit expressions for the augmented two-body PS differential (2.11) and the differential two-body PS (4.36) and integrating over the external Euler angle differential (5.26) the differential n-body PS reads [18]

$$\begin{aligned}d^{3n-7}\Phi_n(m_{a\cdots n})=&\frac{V_2(m_{a\cdots n})}{4\pi}\frac{V_2(\mathfrak{m}_{a\cdots n-1})}{m^2_{a\cdots n-1}}\,\text{đ}\mathfrak{m}^2_{a\cdots n-1}\,\text{đ}\cos\theta^{a\cdots n}_{a\cdots n-2}(\mathfrak{m}_{a\cdots n-1})\\&\prod_{i=b}^{n-2}2\frac{V_2(\mathfrak{m}_{a\cdots i})}{m^2_{a\cdots i}}\,\text{đ}\mathfrak{m}^2_{a\cdots i}\,\text{đ}\phi^{a\cdots i+2}_{a\cdots i-1}(\mathfrak{m}_{a\cdots i},\mathfrak{m}_{a\cdots i+1})\,\text{đ}\cos\theta^{a\cdots i+1}_{a\cdots i-1}(\mathfrak{m}_{a\cdots i}),\end{aligned} \tag{8.4}$$

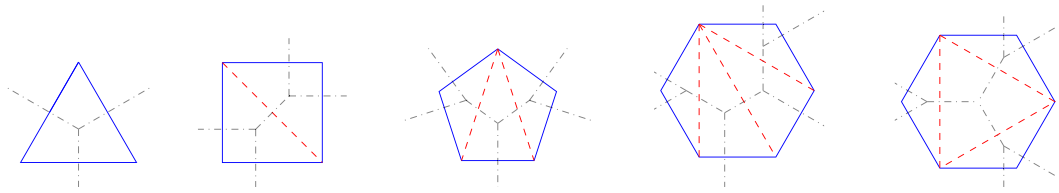
where the areas (4.5) are given in the notation (2.6) and the differentials are normed according to (2.9). In particular this expression recovers the differential three-body PS (5.27), the differential four-body PS (6.23), and the differential five-body PS (7.14) in the parametrization depending on angular variables. The diagram of the n-body PS in this parametrization is depicted in Fig. 11(b). Therefore, the differential n-body PS can be expressed as a product of $n-1$ areas (4.5) together with $n-2$ invariant mass differentials, $n-2$ differential of polar opening angles (5.14), and $n-3$ differentials of azimuthal decay plane angles (6.10). In this parametrization the limits of the integration over the invariant masses can be chosen to be of the simple form (5.29) while the limits of the integration over the angles are trivial (4.30). The optimal set of integration variables can be identified by comparing the diagram in Fig. 11(b) with the Feynman diagram of the corresponding amplitude.

IX. CONCLUSION

We have derived expressions for PSs of an arbitrary number of particles. While the differential PS is especially simple to express in terms of invariant masses the integration in this parametrization is unnecessarily complicated, since generically volumes of four-dimensional parallelotopes appears explicitly and a large number of nontrivial integration limits have to be taken into account. On the other hand a parametrization in terms of a minimal set of invariant masses and fitting polar opening and azimuthal decay plane angles leads to the most readily integrable differential PS. In order to simplify the discussion of such PSs we have developed a graphical depiction that allows one to argue about high dimensional PSs. This graphical description differs from prior proposal [26,27]. In particular when expressed in terms of two-body PSs these diagrams can be interpreted as dual diagrams to tree-level Feynman diagrams consisting of three-particle vertices; see Fig. 12.

ACKNOWLEDGMENTS

This work was supported by the Fundação para a Ciência e a Tecnologia (FCT) under Project No. 2020.03969 .CEECIND/CP1587/CT0014. Jan Hajer acknowledges the hospitality of Stefan Antusch and the Particles and Cosmology group at the University of Basel.



(a) Two-body (b) Three-body (c) Four-body (d) Five-body (e) Five-body

FIG. 12. The PS diagrams can be interpreted as being dual to tree-level Feynman diagrams. The parametrization in terms of differential two-body PSs is particularly well suited to describe Feynman diagram consisting of three-particle interactions. This correspondence is illustrated for two-, three-, and four-body processes in (a)–(c). The two independent configurations that arise when parameterize the five-body PS in terms of angular variables are shown in (d) and (e).

DATA AVAILABILITY

The data that support the findings of this article are openly available [44].

[1] E. Rutherford, The scattering of α and β particles by matter and the structure of the atom, London, Edinburgh, Dublin Philos. Mag. J. Sci. **21**, 669 (1911).

[2] N. F. Mott, The scattering of fast electrons by atomic nuclei, Proc. R. Soc. A **124**, 425 (1929).

[3] V. Weisskopf and E. P. Wigner, Berechnung der natürlichen Linienbreite auf Grund der Diracschen Lichttheorie, Z. Phys. **63**, 54 (1930).

[4] E. Fermi, Quantum theory of radiation, Rev. Mod. Phys. **4**, 87 (1932).

[5] R. P. Feynman, A relativistic cutoff for classical electrodynamics, Phys. Rev. **74**, 939 (1948).

[6] R. P. Feynman, The theory of positrons, Phys. Rev. **76**, 749 (1949).

[7] R. P. Feynman, Space-time approach to quantum electrodynamics, Phys. Rev. **76**, 769 (1949).

[8] N. Byers and C. N. Yang, Physical regions in invariant variables for n particles and the phase-space volume element, Rev. Mod. Phys. **36**, 595 (1964).

[9] E. Byckling and K. Kajantie, n-particle phase space in terms of invariant momentum transfers, Nucl. Phys. **B9**, 568 (1969).

[10] R. Kumar, Covariant phase-space calculations of n-body decay and production processes, Phys. Rev. **185**, 1865 (1969).

[11] E. Byckling and K. Kajantie, Reductions of the phase-space integral in terms of simpler processes, Phys. Rev. **187**, 2008 (1969).

[12] R. A. Morrow, Phase space integral and physical regions for n particles in invariant variables, Ann. Phys. (N.Y.) **57**, 115 (1970).

[13] C. H. Poon, Kinematics of many-particle processes in invariant variables: Physical regions, phase space and all that, Nucl. Phys. **B20**, 509 (1970).

[14] R. Kumar, Covariant phase-space calculations on n-body decay and production processes. II, Phys. Rev. D **2**, 1902 (1970).

[15] E. Byckling and M. L. Whippman, Description of multiparticle phase space in invariant variables, Ann. Phys. (N.Y.) **81**, 49 (1973).

[16] R. Hagedorn, *Relativistic Kinematics*: A Guide to the Kinematic Problems of High-Energy Physics (Benjamin, New York, 1963), ISBN: 978-1-258-26194-8.

[17] G. Källén, *Elementary Particle Physics* (Addison-Wesley, New York, 1964), p. 546, ISBN: 0201035758.

[18] E. Byckling and K. Kajantie, *Particle Kinematics* (John Wiley & Sons, New York, 1973), p. 319, ISBN: 0471128856.

[19] J. Jackson, D. Miller, and D. Tovey, Kinematics, Rev. Part. Phys. **110**, 30001 (2024).

[20] R. A. Morrow, Monte Carlo integration program for the n-particle relativistic phase space integral in invariant variables, Comput. Phys. Commun. **13**, 399 (1978).

[21] R. A. Morrow, Algorithm for the numerical evaluation of the n particle relativistic phase space integral in invariant variables, J. Comput. Phys. **29**, 245 (1978).

[22] C. G. Papadopoulos, PHEGAS: A Phase space generator for automatic cross-section computation, Comput. Phys. Commun. **137**, 247 (2001).

[23] F. Krauss, R. Kuhn, and G. Soff, AMEGIC++ 1.0: A matrix element generator in C++, J. High Energy Phys. 02 (2002) 044.

[24] F. Maltoni and T. Stelzer, MADEVENT: Automatic event generation with MadGraph, J. High Energy Phys. 02 (2003) 027.

[25] O. Mattelaer and K. Ostrolenk, Speeding up MadGraph5_aMC@NLO, Eur. Phys. J. C **81**, 435 (2021).

[26] V. E. Asribekov, Choice of invariant variables for the "many-point" functions, J. Exp. Theor. Phys. **15**, 394 (1962).

[27] H.-J. Jing, C.-W. Shen, and F.-K. Guo, Graphic method for arbitrary n-body phase space, Sci. Bull. **66**, 653 (2021).

[28] S. Mandelstam, Determination of the pion-nucleon scattering amplitude from dispersion relations and unitarity: General theory, Phys. Rev. **112**, 1344 (1958).

[29] P. Srivastava and G. Sudarshan, Multiple production of pions in nuclear collisions, Phys. Rev. **110**, 765 (1958).

[30] C. Møller, General properties of the characteristic matrix in the theory of elementary particles, Matematisk-Fysiske Meddelelser 23.1 (1945).

[31] M. Cannoni, Lorentz invariant relative velocity and relativistic binary collisions, Int. J. Mod. Phys. A **32**, 1730002 (2017).

[32] J. P. Gram, Om Rækkeudviklinger, bestemte ved Hjælp af de mindste Kvadraters Methode, Ph.D. thesis, Andr. Fred. Høst & Son, 1879; Reihenentwicklung nach der Methode der kleinsten Quadrate, J. Reine Angewandte Math. **1883**, 41 (1883).

[33] A. Cayley, A theorem in the geometry of position, Cambridge Math. J. **2**, 267 (1841).

[34] K. Menger, Untersuchungen über allgemeine Metrik, Math. Ann. **100**, 75 (1928).

[35] T. Regge and G. Barucchi, On the properties of Landau curves, Nuovo Cimento **34**, 106 (1964).

[36] R. J. Eden, P. V. Landshoff, D. I. Olive, and J. C. Polkinghorne, *The Analytic S-Matrix* (Cambridge University Press, Cambridge, England, 1966), ISBN: 978-0-521-04869-9.

[37] E. B. Manoukian, On the reversal of the triangle inequality in Minkowski spacetime in relativity, Eur. J. Phys. **14**, 43 (1993).

[38] L. Schläfli, Theorie der vielfachen Kontinuität, *Gesammelte Mathematische Abhandlungen* (Springer, Basel, 1950), Vol. 1, pp. 167–387, ISBN: 978-3-0348-4118-4, 10.1007/978-3-0348-4118-4_13.

[39] Hero of Alexandria, *Metrica. Trans. as Heronis Alexandrini Opera quae supersunt omnia. Vol. 3: Rationes dimetiendi et commentatio dioptrica*, translated by H. Schöne. Bibliotheca Scriptorum Graecorum et Romanorum Teubneriana (Teubner, Leipzig, 1903).

[40] R. H. Dalitz, On the analysis of τ-meson data and the nature of the τ-meson, Phil. Mag. Ser. 7 **44**, 1068 (1953).

[41] K. Yu, D.-M. Li, and J.-J. Wu, Research on the phase space of three- and four-body final states processes, Chin. Phys. C **46**, 083101 (2022).

[42] A. van Hameren and C. G. Papadopoulos, A hierarchical phase space generator for QCD antenna structures, Eur. Phys. J. C **25**, 563 (2002).

[43] R. Frederix and T. Vitos, Leading-colour-based unweighted event generation for multi-parton tree-level processes, J. High Energy Phys. 12 (2024) 201.

[44] J. Hajer, Monte Carlo data used in this publication, 2025, 10.5281/zenodo.17280501.